Sustainable observations of the AMOC: Methodology and Technology

G.D. Mccarthy, P.J. Brown, C.N. Flagg, G. Goni, L. Houpert, C.W. Hughes, R. Hummels, M. Inall, K. Jochumsen, K.M.H. Larsen, et al.

AGU100 ADVANCING EARTH AND SPACE SCIENCE

Reviews of Geophysics

REVIEW ARTICLE
10.1029/2019RG000654

Special Section:
Atlantic Meridional Overturning Circulation: Reviews of Observational and Modeling Advances

Sustainable Observations of the AMOC: Methodology and Technology

G. D. McCarthy[1], P. J. Brown[2], C. N. Flagg[3], G. Goni[4], L. Houpert[5,2], C. W. Hughes[6,2], R. Hummels[7], M. Inall[5], K. Jochumsen[8], K. M. H. Larsen[9], P. Lherminier[10], C. S. Meinen[4], B. I. Moat[2], D. Rayner[2], M. Rhein[11,12], A. Roessler[11,12], C. Schmid[4], and D. A. Smeed[2]

[1]ICARUS, Department of Geography, Maynooth University, UK, [2]National Oceanography Centre, Southampton, UK, [3]Marine Science Research Center, State University of New York at Stony Brook, Stony Brook, NY, USA, [4]Atlantic Oceanographic and Meteorological Laboratory, Miami, FL, USA, [5]Scottish Association for Marine Science, Oban, UK, [6]School of Environmental Sciences, University of Liverpool, Liverpool, UK, [7]GEOMAR Helmholtz Centre for Ocean Research Kiel, Kiel, Germany, [8]Federal Maritime and Hydrographic Agency, Hamburg, Germany, [9]Faroe Marine Research Institute, Faroe Islands, [10]Ifremer, Université Brest, CNRS, IRD, LOPS, IUEM, F-29280, Plouzané, France, [11]Institute for Environmental Physics, Bremen University, Bremen, Germany, [12]Center for Marine Environmental Sciences MARUM, Bremen University, Bremen, Germany

Key Points:
- The AMOC is a system of ocean currents that move heat and carbon around the planet and is predicted to decline in the future
- The AMOC has been directly measured since the 2000s, but we now have observation systems in place that can verify a future decline
- We look at how these systems might develop in the future and consider how they might fit in an optimized Atlantic observing system

Correspondence to:
G. D. McCarthy,
gerard.mccarthy@mu.ie

Citation:
McCarthy, G. D., Brown, P. J., Flagg, C. N., Goni, G., Houpert, L., Hughes, C. W., et al. (2020). Sustainable observations of the AMOC: methodology and technology. *Reviews of Geophysics*, *58*, e2019RG000654. https://doi.org/10.1029/2019RG000654

Received 29 APR 2019
Accepted 18 NOV 2019
Accepted article online 23 NOV 2019

Abstract The Atlantic Meridional Overturning Circulation (AMOC) is a key mechanism of heat, freshwater, and carbon redistribution in the climate system. The precept that the AMOC has changed abruptly in the past, notably during and at the end of the last ice age, and that it is "very likely" to weaken in the coming century due to anthropogenic climate change is a key motivation for sustained observations of the AMOC. This paper reviews the methodology and technology used to observe the AMOC and assesses these ideas and systems for accuracy, shortcomings, potential improvements, and sustainability. We review hydrographic techniques and look at how these traditional techniques can meet modern requirements. Transport mooring arrays (TMAs) provide the "gold standard" for sustained AMOC observing, utilizing dynamic height, current meter, and other instrumentation and techniques to produce continuous observations of the AMOC. We consider the principle of these systems and how they can be sustained and improved into the future. Techniques utilizing indirect measurements, such as satellite altimetry, coupled with in situ measurements, such as the Argo float array, are also discussed. Existing technologies that perhaps have not been fully exploited for estimating AMOC are reviewed and considered for this purpose. Technology is constantly evolving, and we look to the future of technology and how it can be deployed for sustained and expanded AMOC measurements. Finally, all of these methodologies and technologies are considered with a view to a sustained and sustainable future for AMOC observation.

Plain Language Summary The Atlantic Meridional Overturning Circulation (AMOC) is a system of ocean currents (sometimes known as the Gulf Stream System or the Great Ocean Conveyor Belt) that is important because of how it moves heat and carbon around the planet. Due to human-induced climate change, the AMOC is predicted to weaken substantially, with adverse impacts for regions dependent on the supply of warmth from the AMOC, including northwest Europe. Surprisingly, given its importance, the AMOC has only been directly measured for the last decade or so. We now have observation systems in place that can verify a future decline in the AMOC, if it happens. In this paper we review these observation systems in terms of the technology and methodology used. We look at how these systems might develop in the future, including covering any gaps that might exist, and consider how they might fit in an integrated and optimized Atlantic observing system.

1. Introduction

The Atlantic Meridional Overturning Circulation (AMOC) is a system of ocean currents that exchanges waters horizontally and vertically across vast distances within the Atlantic. The AMOC consists primarily of two overturning cells in latitude-depth space (Figure 1). Each cell is associated with deep water formed in the high latitude North Atlantic and bottom water formed in the Southern Ocean, respectively, that we will refer to as the primary and deep overturning cells. The AMOC transports heat, freshwater, carbon, and nutrients around the Atlantic. It is an important factor in decadal climate variations (Zhang et al.,

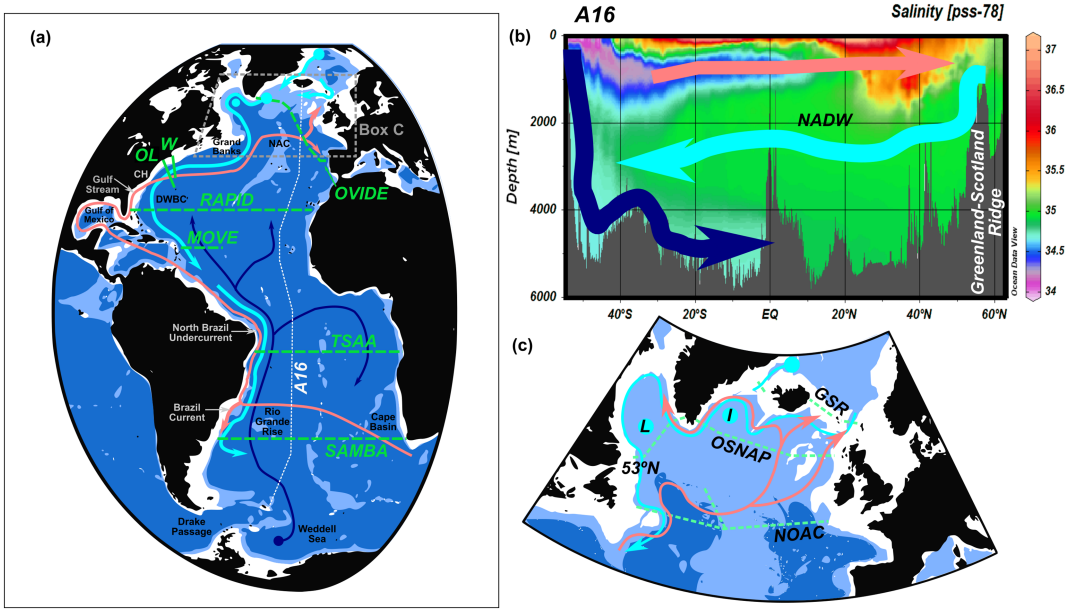

Figure 1. (a) Idealized pathways of the main water masses of the AMOC. The warm, shallow upper branch or the primary AMOC cell is shown in pink. The cold, deep return flow of North Atlantic Deep Water (NADW) is shown in cyan. The pathways of Antarctic Bottom Water (AABW) are shown in navy blue. Sources of deep water are shown with open circles. (b) The primary and deep overturning cells in latitude-depth space. These are superimposed on salinity section along the A16 WOCE hydrographic line (hydrographic track shown in a). The warm, shallow branch is approximately confined to the upper 1,000 m; NADW is identified with a broad salinity signature between 2,000 and 4,000 m. AABW is confined to depths greater than 4,000 m. (c) Zoom of (a), north of 40°N, showing the sources of NADW north of the Greenland-Scotland Ridge (GSR) and in the Labrador (L) and Irminger (I) Seas. AMOC observing lines referred to in the text are indicated with green dashed lines in (a) and (c). CH = Cape Hatteras, OL = Oleander Line, W = Line W, NAC = North Atlantic Current, DWBC = Deep Western Boundary Current.

2019), northern and southern hemisphere atmospheric patterns (Jackson et al., 2015; Lopez et al., 2016; McCarthy, Gleeson, et al., 2015) and to the rate of sequestration of anthropogenic carbon in the deep ocean (Steinfeldt et al., 2009). The convolutions of the Earth's geological past point to large, chaotic oscillations in the AMOC (Dansgaard et al., 1993). The convolution ongoing in the modern climate system is of a different nature being largely man-made (Stocker et al., 2013). Consensus among climate projections from the 5th Coupled Model Intercomparison Project (CMIP5) is that the AMOC is *very likely* to decline due to anthropogenic climate change in the coming century. A collapse is thought to be unlikely but not impossible (Stocker et al., 2013). In light of the importance of the AMOC and urgency in terms of its future evolution, efforts are ongoing to observe the AMOC. This paper reviews the main technologies and methodologies that have been used to observe the AMOC, with a focus on observations of the circulation itself and the associated heat, freshwater, and carbon transports rather than on the processes that maintain the AMOC (such as deep water formation and mixing).

To understand the technological and associated methodological needs, a brief description of the AMOC and certain AMOC observation systems referred to in the text is first necessary (Figure 1). The primary overturning cell associated with the AMOC can be described in a simplified manner as follows. Warm water enters the Atlantic at its southern boundary from the Indian Ocean, near the SAMBA array at 34.5°S where it is measured using pressure equipped inverted echo sounders (PIES) and other moorings (Meinen et al., 2018). This so-called warm water path consists of leakage from the Indian Ocean, often in the form of Agulhas Rings (Donners & Drijfhout, 2004; Gordon, 1986; Laxenaire et al., 2018). A slightly cooler pathway, the so-called “cold path,” brings intermediate waters into the Atlantic via Drake Passage. These waters also transit the Cape Basin beneath the warmer Indian Ocean waters before turning northward (Rintoul, 1991). Together, these two water masses represent the upper limb of the primary overturning cell (which is all warm relative to the deeper ocean waters), and it can be traced westward across the South Atlantic where a bifurcation in the flow occurs north of the Rio Grande Rise, off the coast of Brazil near 20°S. From here,

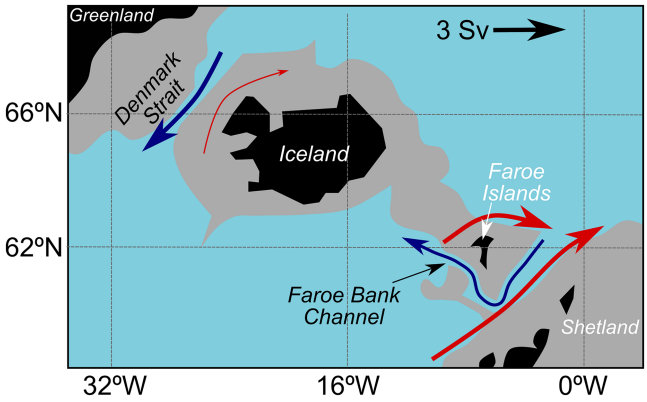

Figure 2. Main flows across the Greenland-Scotland Ridge. Deep overflows through the Denmark Strait and Faroe Bank Channel are shown with blue arrows. Warm, shallow inflow is indicated with red arrows. Arrows are approximately scaled proportion to transport. Gray topography is shallower than 750 m. Adapted from Østerhus et al., 2019.

the Brazil Current branches southward as the western boundary current of the South Atlantic subtropical gyre, and the North Brazil Undercurrent flows to the north, where moored current meter observations exist at 11°S that observe this northward flow and the southward flowing Deep Western Boundary Current (DWBC), the latter predominantly in the form of deep eddies of NADW (Hummels et al., 2015). This 11°S mooring array has been extended across the basin as the Tropical South Atlantic Array (TSAA). On crossing the equator, warm waters move northward through the Caribbean and Gulf of Mexico, eventually becoming recognizable as the Gulf Stream. The Gulf Stream has popularly, if inaccurately, been synonymous with the AMOC (Maury, 1855). Confined to the Straits of Florida between Miami and the Bahamas, where it is known as the Florida Current, this western boundary current flows northward close to the coast where it is monitored by long-term observations based on subsurface cable measurements since 1982—the longest continuous time series of any western boundary current (Meinen et al., 2010). This Florida Current cable measurement system forms an integral part of the RAPID/MOCHA/WBTS array (hereafter the RAPID array), the first basinwide mooring array (current meters, moored conductivity-temperature-depths, CTDs, and bottom pressure recorders, BPRs), designed to measure the strength of the AMOC (Cunningham et al., 2007). Farther north, the Gulf Stream separates from the North American coast at Cape Hatteras. A volunteer observing ship (VOS), the container ship *Oleander*, has been observing the flow of the Gulf Stream between New Jersey and Bermuda using an acoustic Doppler current profiler (ADCP) (Flagg et al., 1998) since 1992. The extended Gulf Stream reattaches to the continental shelf near the Grand Banks and turns northward and crosses the NOAC mooring array at 47°N (PIES, current meters) that has been extended in 2016 to a basinwide array (Mertens et al., 2014) and the repeat hydrographic line OVIDE (Mercier et al., 2015). Shortly thereafter the flow, known now as the North Atlantic Current (NAC) at this point, turns eastward toward Europe. In the eastern basin, the NAC divides between flow to the south to close the subtropical gyre, and northward flow into the eastern subpolar gyre. This flow into the eastern subpolar gyre then divides again between being incorporated in the North Atlantic subpolar gyre and flow across the GSR, predominantly between Iceland and the Shetland Islands (Figure 2), where it is observed by moored current meters (Berx et al., 2013; Hansen et al., 2015). The branch that circulates around the subpolar gyre is observed by the basinwide OSNAP array (current meters, moored CTDs, and gliders) (Lozier et al., 2017).

The densest elements of the deep, cold, return flow of this primary AMOC cell originate in the cold, deep waters formed north of the GSR that enter the broader North Atlantic circulation through overflows across the GSR. This deep overflow can only cross the GSR at two deep points: the Faroe-Bank Channel (Hansen et al., 2016) and the Denmark Strait (Jochumsen et al., 2017) (Figure 2). These overflows have been observed with current meter moorings since the mid-1990s. An additional source of the deep branch is associated with the deep convection regions of the Labrador (Rhein et al., 2017, 2011; Yashayaev & Loder, 2016) and Irminger Seas (de Jong et al., 2018). These processes and the technologies that observe them are not the focus of this review so we limit our attention to observations of the ocean circulation associated with the AMOC and the heat, freshwater, and, most recently, carbon transport associated with it. We will refer to the water masses of this branch collectively as NADW.

NADW exits the subpolar gyre at its southwestern boundary, passing the 53°N array that forms a key part of OSNAP West (Zantopp et al., 2017), to feed the DWBC of the subtropical North Atlantic (Figure 1). In doing so, NADW passes the locations of the NOAC (Mertens et al., 2014), Line W (Toole et al., 2017), and the RAPID arrays again. At 16°N, the MOVE array (moored CTDs) estimates the southward flow of NADW (Send et al., 2002). In the South Atlantic, this deep branch is observed at 11°S and 34.5°S by the TSAA and SAMBA arrays, respectively (Hummels et al., 2015; Meinen et al., 2013). This southward deep flow is not a continuous current along the boundary in either the North Atlantic (Bower et al., 2009) or in the South Atlantic (Dengler et al., 2004) as is simplistically depicted in Figure 1, but property extrema associated with recently ventilated NADW (particularly high dissolved oxygen and chlorofluorocarbons CFCs) are

identifiable from the subtropical North Atlantic to the southern boundary of the South Atlantic (Rhein et al., 2015).

The deep overturning cell is also a feature of the AMOC. This is driven by the densest of deep waters formed in the Southern Ocean, in particular, the Weddell Sea: Antarctic Bottom Waters (AABW). The path of AABW is highly dependent on the abyssal topography, being constrained to flow west of the Mid-Atlantic Ridge apart from where deep fractures in the ridge allow AABW to enter successive basins to the north (Figure 1). Distinctive high silicate values of AABW are noted as far as the subpolar North Atlantic. Efforts to measure this flow have concentrated on constriction points such as the deep current meter measurements in the Vema Channel, close to the Rio Grande Rise in the South Atlantic (Zenk & Morozov, 2007) or hydrographic estimates of the flow using shipboard hydrography (Morozov et al., 2018) or dynamic height moorings (Frajka-Williams et al., 2011).

This brief description of the AMOC highlights some of challenges in observing it. However, the laminar, linked flow depicted in Figure 1 is a great simplification. It does not depict the mesoscale ocean variability that is a feature of separated western boundary currents (e.g., Andres, 2016), DWBCs (Bower et al., 2009; Dengler et al., 2004), Agulhas leakage (Biastoch et al., 2008), and the open ocean itself (Wunsch, 2008). This description also neglects the multiple pathways associated with currents, such as the NAC (Rhein et al., 2019; Roessler et al., 2015), recirculations or quasi-stationary meanders and eddies that are also a feature of both upper and deep ocean currents (Meinen et al., 2013; Mertens et al., 2014; Rhein et al., 2019). The depiction of a connected Atlantic-wide AMOC in Figure 1 implies a coherence of ocean transport which does not exist. For example, in the North Atlantic the subtropical and subpolar gyres are believed to be dominated by differing timescales of variability (Bingham et al., 2007; Williams et al., 2014). All of these complex challenges need to be accounted for when making observations of the AMOC. Consequently, there are different motivations and rationales for the multiple AMOC observing systems that currently exist and the methods and technology used to measure the AMOC vary depending on the nature of the circulation and the practicalities of observation at a given location and for a given program. This paper reviews how the AMOC is measured focusing on the technology and methodology required to do so.

The paper is organized as follows: Sections 2–4 focus on three observing systems that generate estimates of the AMOC (shipboard hydrography, TMAs, and remote sensing) and are organized approximately chronologically. Section 5 focuses on technology and methodology that is either not employed or employed in a limited sense in AMOC observing systems. We believe that the technologies described here have greater exploitation potential in terms of AMOC observing. Section 6 describes observational gaps—both geographical and parametric. The final section aims to summarize and rationalize the AMOC observing systems that currently exist and discusses future outlooks.

2. Shipboard Hydrography

Shipboard hydrography is the oldest method of measuring the AMOC. Many early ocean expeditions followed long tracks of exploration such as the Challenger expedition in 1872–1876. These were soon organized into the recognizable zonal or meridional hydrographic sections. (Wust, 1935) led a series of zonal hydrographic sections in the South Atlantic in the 1920s and 1930s that included early estimates of heat transport. These were not published as the heat transport "flew in wrong direction" (personal communication from Admiral E. K. E. Noodt to Professor Henry Stommel). Equatorward heat transport was not considered correct as the principle of redistribution of heat away from the equator prevailed. We now know that heat is transported equatorward in the South Atlantic due to the AMOC (Bryden & Imawaki, 2001) and this comment must mark one of the earliest indications of the nature of the AMOC. Early qualitative estimates of the AMOC from property distributions supported a value of a "weak" overturning or approximately 7 Sv, which prevailed from Sverdrup et al. (1942) to Worthington (1976). The early 1980s saw a change in estimates of the AMOC with the analysis of North Atlantic hydrographic sections of Bryden and Hall (1980) and Hall and Bryden (1982) that saw the now accepted vigorous overturning estimates of approximately 18 Sv with an associated heat transport of 1.3 PW in the subtropical North Atlantic. The WOCE experiments of 1990s saw systematic hydrographic sections and analysis of global circulation on an unprecedented scale, leading to the global estimates of ocean circulation by Macdonald and Wunsch (1996) and Ganachaud and Wunsch (2003).

The workhorse of modern shipboard hydrography is the CTD that provides estimates of a range of parameters. Of particular interest in this review are the physical parameters of salinity, temperature, pressure, and velocity. Temperature is possibly considered the most stable variable measured by the CTD, with accuracies of 0.001 °C and stability of 0.0002 °C per month (Sea Bird Electronics, 2014). Pressure estimates on shipboard CTDs typically use Digiquartz pressure sensor that can provide accuracies of 0.015% of full ocean depth. A similar but higher precision Digiquartz pressure sensor is also employed in BPRs (section 5.2) and pressure inverted echo sounders, whereas economical strain gauge sensors are used on Argo floats and moored CTDs. Salinity can be measured to an accuracy of 0.003 g/kg with a stability of 0.003 g/kg/month. Pumped CTD sensors are crucial to this accuracy. Bottle samples of salinity are still essential for the accurate calibration of CTD salinity, traceable to standard seawater, which is necessary for estimations of ocean circulation. For example, McCarthy, Smeed, et al. (2015) highlighted that a bias of 0.003 g/kg in salinity resulted in a bias in the AMOC estimate at 26°N of 0.7 Sv, a large contributor to the total 1 Sv accuracy of the RAPID estimate. Hence, the uncorrected drift of the CTD salinity sensor could be expected to give a 1 Sv bias to an AMOC estimate based on a 6-week hydrographic cruise in the subtropical North Atlantic.

Modern hydrographic expeditions are frequently equipped with ADCPs technology both fixed to the ship (examples discussed in section 5.1) or lowered on the CTD package (lowered acoustic Doppler current profiler, LADCP). These provide estimates of the absolute velocity profile using the principle of Doppler shift from scatterers in the water column. These scatterers are typically zooplankton or suspended particles in the water column. In the absence of sufficient quantities of these scatterers in the water, ADCP technology struggles.

Estimation of meridional transport by hydrographic data relies on the calculation of geostrophic transport/velocity from profiles of temperature, salinity, and pressure. The meridional transport as a function of depth, $\boldsymbol{T(z)}$, between two points, w and e (west and east) is given by

$$T(z) = \int_w^e v(z,x)\, dx \tag{1}$$

where $\boldsymbol{v}$ is the meridional velocity. To a good approximation, over appropriate length and timescales, velocity in the ocean is geostrophic:

$$\rho f \mathbf{k}\times\mathbf{v} = -\nabla p, \tag{2}$$

where $\boldsymbol{\rho}$ is density, $\boldsymbol{p}$ is pressure, $\boldsymbol{f}$ is the Coriolis parameter, and

$$\mathrm{v} = u\mathbf{i} + v\mathbf{j} + w\mathbf{k}$$

is the velocity in the zonal, meridional, and vertical directions. Considering only meridional velocities at a fixed latitude, the geostrophic meridional velocity can be expressed as

$$f_0 v = \frac{1}{\rho}\frac{\delta p}{\delta x}. \tag{3}$$

Substituting (3) into (1) gives

$$T(z) = \int_w^e v(z)\, dx = \frac{1}{\rho_0 f_0}\left[p_e[z] - p_w[z]\right], \tag{4}$$

where

$$p(z) - p(z_r) = \int_z^{z_r} \rho g dz. \tag{5}$$

The subscript, r, refers to a reference level. Hydrostatic pressure in the ocean is more commonly defined in terms of dynamic height, $\boldsymbol{\Phi}$, and, in the idealized case of vertical sidewalls, equation (4)s can be simplified as

$$T(z) = \frac{1}{f_0}\left[\Phi_e[pp_r] - \Phi_w[pp_r]\right], \tag{6}$$

Dynamic height can be calculated as the vertical integral of specific volume anomaly, $\boldsymbol{\alpha}$, which is the reciprocal of density:

$$\Phi(pp_r) = \int_{p_r}^{p} \alpha \, dp = \int_{p_r}^{p} \frac{dp}{\rho}. \quad (7)$$

In practice, due to traditional reasons that no longer apply with modern computing power, dynamic height anomaly and specific volume anomaly are typically calculated (IOC et al., 2010).

An unknown for the calculation of geostrophic transport is the reference level velocity or, equivalently, the reference level dynamic height. Initial values for a level of no motion can be chosen between water masses that flow in opposite directions or at the deepest common level between stations. For example, between northward flowing Antarctic Intermediate Water and southward flowing NADW in the subtropical North Atlantic. However, many observations have shown that levels of no motion either do not exist in a time-varying sense and they need not correspond directly to a given water mass definition nor to the deepest common level, leading to the need to refine this assumption. For basinwide hydrographic sections, a constraint of zero mass transport across the section may be imposed (Bryden & Hall, 1980) or a constraint of fixed throughflow can be imposed. For example, the Labrador Sea is a partial basin with a known inflow of approximately 1.6 Sv southward through its northern boundary at the Davis Strait (Curry et al., 2014). This constraint can be applied to adjust geostrophic transports at the southern exit of the Labrador Sea (Holliday et al., 2018). Direct velocity estimates from ship or lowered ADCP may be used to constrain the geostrophic velocity (Hernández-Guerra et al., 2014; Holliday et al., 2018; Mercier et al., 2015). A combination of these constraints is generally used to make estimates of the full geostrophic velocity section from individual hydrographic sections.

If a number of hydrographic sections are available that enclose an ocean section, box inverse methods may be applied to solve the reference level issue (Wunsch, 1996). This method uses the constraint of conservation of conservative properties, such as mass/volume, salinity, or other conservative tracers to solve for the unknown reference level velocity. It was employed in the global circulation studies of Macdonald and Wunsch (1996) and Ganachaud and Wunsch (2003) and in recent estimates of the AMOC by Hernández-Guerra et al. (2014) and Fu et al. (2017).

Once the full velocity field is established, defining the AMOC becomes straightforward. The AMOC is generally defined as the maximum of the overturning stream function:

$$\mathrm{AMOC} = max(\Psi(z)) = max\left(\int_0^{-H} T(z)\, dz\right), \quad (8)$$

where $\boldsymbol{\Psi}$is the overturning stream function and $-H$ is the full depth of the ocean. The first observational descriptions of the AMOC as a stream function were due to Talley et al. (2003). In the definition followed here, depth was used as the vertical coordinate but density is also used as a vertical coordinate depending on the application. Defining the overturning in density space is particularly widely deployed in the subpolar North Atlantic where the AMOC-associated heat transport is controlled by the warm water entering on the east and cold water exiting on the west (Lozier et al., 2019). These pathways are not distinct in depth but are distinct in density and hence a definition of

$$AMOC = max\left(\Psi'(\rho)\right) = max\left(\int_{min(\rho)}^{max(\rho)} T'(\rho) d\rho\right).$$

Original estimates of the AMOC from hydrographic sections were focused on establishing the mean AMOC. Current interest in the AMOC is motivated by how the AMOC may be changing, in particular in response to anthropogenic climate change. Bryden et al. (2005) published estimates from five hydrographic sections that indicated a 30% decline in the overturning circulation at 24°N. This analysis was soon followed by sustained observations of the AMOC at approximately the same latitude using a TMA (section 3) that showed the variability discussed by Bryden et al. (2005) could be seen over the course of a number of weeks (Cunningham et al., 2007). The identification of a strong seasonal cycle in the AMOC in the RAPID data led to a revision of the shipboard hydrographic estimates (Kanzow et al., 2010) and aliasing a higher frequency signal could not be ruled out. The existence of these higher frequency signals also highlights the asynopticity issues for use of hydrographic cruises for AMOC estimates. Transbasin cruises across wider parts of the basin typically take up to 6 weeks to complete, during which time the ocean is changing.

So what is the future of hydrographic estimates of the AMOC in the era of sustained observations? The estimates of Bryden et al. (2005) were in the subtropical North Atlantic. This region is known for strong interannual variability in circulation, which is a contrast to the subpolar North Atlantic where the circulation is believed to vary more slowly (Bingham et al., 2007; Williams et al., 2014). In the subpolar North Atlantic, the OVIDE project has made estimates of the AMOC in density space in a series of shipboard hydrographic sections. In contrast to the picture of interannual variability swamping the hydrographic estimate, the OVIDE repeat hydrography project (Figure 1) has shown that decadal variability in the AMOC is detectable using shipboard hydrographic estimates in conjunction with satellite and Argo data (Mercier et al., 2015). This indicates the continued utility of shipboard hydrography for estimating the AMOC in the appropriate circumstances.

3. Transport Moorings Arrays

3.1. Existing AMOC Observing Systems

While mooring arrays had previously been used to calculate mass transports of individual currents or flows such as at the GSR (Østerhus et al., 2005), the concept of a truly transbasin array designed to monitor the complete meridional overturning circulation only emerged after 2000. Model simulations suggested that there is large variability of the AMOC on daily to seasonal time scales that could mask longer-term variability if observations were made only at a few snapshots in time such as (Bryden et al., 2005) results discussed in the previous section. Thus, to monitor long-term observations, continuous observations from purposefully designed arrays were needed (Hirschi et al., 2003).

At the time of writing there are five basinwide mooring arrays measuring the AMOC: The OSNAP array in the northern boundary of the subpolar North Atlantic, the NOAC array at the southern boundary of the subpolar North Atlantic at 47°N, RAPID at 26°N in the subtropical North Atlantic, the TSAA array at 11°S and the SAMBA array at 34°S in the South Atlantic. In addition, there are a number of other arrays that measure DWBC transports (Send et al., 2002; Zantopp et al., 2017). Many additional systems monitor vital components of the overturning such as the GSR array that incorporates measurements of Atlantic water inflow to the Greenland-Iceland-Norwegian Seas (Berx et al., 2013; Hansen et al., 2010) and deep overflow water through the Denmark Straits (Jochumsen et al., 2017) and Faroe Bank Channel (Hansen et al., 2016).

The first deep water moorings were designed to carry current meters (Richardson et al., 1963, see section 3.3 for more detail) that provide measurements of water speed and direction at the locations of instruments. Arrays of such instruments can be used to estimate volume transports, but the high-spatial resolution of instruments required would necessitate an unfeasibly large number of instruments and moorings to measure basinwide transports. Fortunately, throughout much of the ocean, on time scales of a few days or more, ocean currents are to good approximation in geostrophic balance (Bryden et al., 2009). Thus, as we have seen for shipboard hydrographic profiles, instead of measuring the velocity everywhere between two points, it suffices to measure the pressure at the end points only. In a (1/12)° ocean model study using a simulated transbasin observing array, Sinha et al. (2018) considered the errors in the estimation of the AMOC that arise from the geostrophic assumption. In the model, neglect of ageostrophic motion, other than the Ekman layer, leads to a potential mean bias of the order of 0.5 Sv and potential time varying errors with a standard deviation of about 0.1 Sv.

BPRs have been used to examine the variability of basinwide geostrophic transport (Kanzow et al., 2009), and their use is discussed further in section 5.2. However, it is not yet possible to measure the absolute value of pressure and absolute level of the instrument with sufficient accuracy to determine mean transport, and instrument pressure drift can complicate the analysis of variability on time scales longer than a few months.

An alternative approach is to calculate dynamic height profiles in an analogue to the approach with shipboard hydrographic section data. The required profile of density may be determined from temperature and salinity measurements at a number of depths on a mooring (sections 2 and 3.2), or, in some cases, it may be estimated from travel time measurements from an inverted echo sounder on the seafloor combined with hydrography-derived lookup tables or transfer functions.

The same issue occurs with moored estimations of transport based on dynamic height as does with shipboard measurements: determination of the reference velocity. A number of different approaches can be used to estimate the reference velocity values. Similar approaches can be employed to shipboard hydrographic data in determining the reference level velocity. The main difference is that the estimates of the reference velocity need to be continuous in time. If the reference level is chosen to be the sea surface then altimetry may be used to estimate surface transport (e.g., Berx et al., 2013) although sea surface height (SSH) variations include both barotropic and baroclinic contributions, which can be difficult to untangle in the absence of other continuous-in-time measurements of one or the other component.

Two North Atlantic transbasins arrays, RAPID 26°N and OSNAP, each use a combination of techniques with some parts of the transport being quantified directly by current measurements, and other parts being determined indirectly by geostrophic estimates. For each of these arrays, an additional time-varying adjustment is made to ensure that there is no net transport by adding a vertically uniform compensation velocity across the whole basin (e.g., Kanzow et al., 2007). The South Atlantic SAMBA array described by Meinen et al. (2018); Meinen, Speich, et al. (2013) uses geostrophically derived transports and applies a time-varying reference velocity based on bottom pressure differences and a time mean from a numerical model; the AMOC estimates to date from SAMBA have only involved the upper limb of the primary AMOC cell. For all three arrays the ageostrophic Ekman flow is derived from wind stress estimated by reanalysis products such as ERA-interim (Dee et al., 2011). Arrays that monitor the DWBCs also use a combination of geostrophic estimates and direct current measurements.

3.2. Dynamic Height Moorings

The importance of the calculation of dynamic height in the calculation of an AMOC estimate is emphasized in equations (6) and (8). Hydrostatic pressure is usually expressed as dynamic height, which has units of square meters per square second, and is evaluated by integrating the specific volume anomaly, α, from the reference pressure (equation (7)). McCarthy, Gleeson, and Walsh (2015) found that changing the equation of state used to evaluate the specific volume anomaly from EOS-80 to TEOS-10 (IOC et al., 2010) reduced the estimated AMOC at 26°N by about 2% (0.4 Sv). This results from the spatial variability of silicate concentration that is taken account of when calculating absolute salinity in TEOS-10. The impact of the changed equation of state on transport evaluated at a number of sections is evaluated by Almeida et al. (2018)

The errors that can arise in the calculation of dynamic height have been considered by Johns et al. (2005), McCarthy, Gleeson, and Walsh (2015), and Williams et al. (2015) There are two principal sources of error: instrument calibration and that which arises from the distribution of instruments.

Given typical instrument errors and noting that instrument errors are not expected to be correlated between different instruments, McCarthy, Gleeson, and Walsh (2015) concluded that, when there are a large number of instruments on a mooring, instrument error is not expected to be significant. However, a more important error can arise from the calibration of instruments. CTD sensors used on moorings are normally calibrated at sea by performing a calibration profile in which the instruments are attached to a CTD and compared with a more accurate instrument which is in turn calibrated by taking water samples for analysis of salinity. Thus, it is highly likely that all instruments on a mooring will have the same calibration error and could be biased relative to another mooring. McCarthy, Gleeson, and Walsh (2015) showed that for the RAPID 26°N array a salinity bias of 0.003 would lead to an AMOC error of almost 1 Sv. A similar accuracy of 1 Sv is quoted for the OSNAP AMOC estimates (Lozier et al., 2019). This underlines the great importance of accurate instrument calibration.

To evaluate the integral of equation (5), it is necessary to interpolate between the instrument levels. Johns et al. (2005) describe a method that uses the climatological gradients of temperature and salinity. An alternative approach in which anomalies relative to climatological profiles are used is described by Williams et al., (2015). In both cases the errors are proportional to the second derivative of the profile and so the separation between instruments is chosen to minimize this error with reduced spacing between instruments in the upper part of the water column.

To minimize the risk of damage, moorings often do not extend to the surface (McPhaden et al., 2010). For example, on the RAPID 26°N array most moorings are designed to have the uppermost instrument 50 m below the surface. Additionally, strong currents may "knock down" moorings dragging the instruments

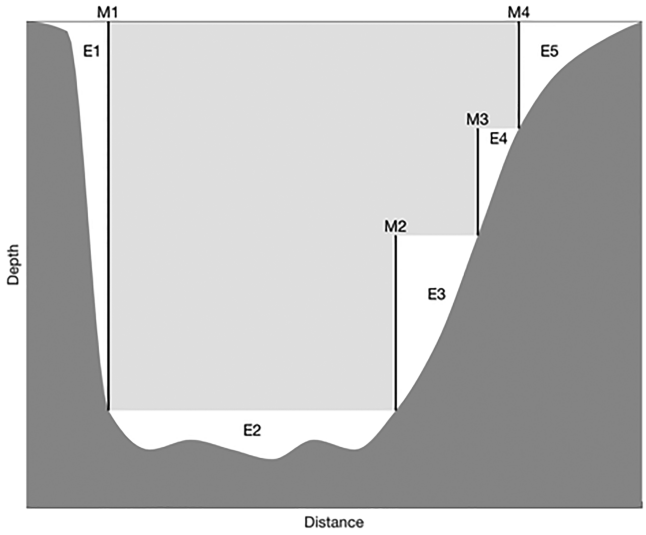

Figure 3. Schematic of a dynamic height mooring array. There are four moorings M1, M2, M3, and M4. From these, geostrophic transport can be evaluated in the shaded area. There are 5 unsampled regions labeled E1, E2, E3, E4, and E5.

deeper. Thus, it is necessary to extrapolate the profile to the surface. Initially, the RAPID 26°N array used a linear extrapolation of dynamic height. This is equivalent to assuming that temperature and salinity are constant above the uppermost instrument, as tested by Williams et al. (2015). However, a model study by Haines et al. (2013) suggested that, in the summer months when there is strong stratification near the surface, this could lead to a bias of up to 1.5 Sv in the transport in the upper 150 m. Williams et al. (2015) showed that this error could be reduced by making use of sea surface temperature measurements and linearly interpolating temperature up to the surface. McCarthy, Gleeson, and Walsh (2015) added quadratic and cubic terms into the extrapolation of dynamic height. The coefficients for these terms were derived from historical profiles in the same region at the same time of year. When tested on full depth profiles, McCarthy, Gleeson, and Walsh (2015) found that this method was more accurate than that based on sea surface temperature when the uppermost instrument was deeper than 100 m. The magnitude of the extrapolation error depends on the location, time of year, and depth of the uppermost instrument, but when the latter is no more than 200 m, then McCarthy, Gleeson, and Walsh (2015) found the transport errors is on average less than 0.5 Sv at 26°N.

If the cross section of the ocean were rectangular, then just two dynamic moorings would be needed to measure the meridional transport at all depths: one adjacent to each boundary. For the real ocean with a sloping seafloor, multiple moorings are needed, as illustrated in Figure 3. In the schematic in Figure 3, only the moorings at the far ends of the array extend to the surface. In contrast the moorings further down the slope only need extend up to the bottom of the next mooring up the slope. An arrangement like this is used on the eastern boundary of the RAPID array (McCarthy, Gleeson, & Walsh, 2015). Transport between two dynamic moorings can only be evaluated down to the maximum depth of the shallowest mooring. There is thus an unsampled region often referred to as a bottom triangle. Design of an array requires a compromise between the cost associated with a larger number of moorings and the errors from having too few moorings. Baehr et al. (2004) note that some prior knowledge of the transport is needed to design an array so that the errors from the missing triangles are not too large, and for this model studies and hydrographic sections are very valuable. McCarthy, Gleeson, and Walsh (2015), using an eddy resolving model, made a careful analysis of the errors arising from unsampled regions and found that for an array configuration similar to that of the RAPID 26°N array unsampled regions over the mid-Atlantic ridge and the deep eastern boundary resulted in a bias of the order of 0.3 Sv for the AMOC, but the bias in the value of the stream function at deeper levels could be up to 1 Sv.

An additional consideration when designing an array is the risk of mooring loss. All of the transbasin arrays have some amount of redundancy so that in the event of a single mooring loss the impact on the accuracy of the AMOC calculation would not be too large. This is particularly important for upper layers that contribute most to the variability of the AMOC (McCarthy et al., 2017).

3.3. Current Meter Moorings

As we have seen, the first moorings were designed to carry current meters. However, in the context of AMOC observing, due to the costs of an entire transbasin current meter array, several basinwide arrays consist of a current meter array only near ocean boundaries, where the transports ideally occur in well-defined current cores, and estimate the other components of the AMOC based on dynamic height moorings or inverted echo sounders. Hence, this section focuses on these current meter arrays, present (or formerly present) at, for example, 53°N (Zantopp et al., 2017), Line W (Toole et al., 2017), MOVE at 16°N (Send et al., 2011), and 11°S (Hummels et al., 2015).

Design begins with the selection of the right location for a current meter array. The research questions that motivate the observations decide the large-scale setting for the array (e.g., the subpolar gyre or the tropics). Existing knowledge about this region needs to be evaluated before installing the instruments. A special focus on understanding branching or merging of flows is necessary to select the best place for the array at the

boundary. It should be placed downstream of known flow convergences (e.g., 53°N, at the exit of the Labrador Sea) or recirculations (11°S, north of the bifurcation of the South Equatorial Current) in order to get the most complete picture of the meridional Western Boundary Circulation System and its variability for a certain regime. It is preferable to find a location where the flow is mostly advective, rather than a turbulent region. This can be hard to assess a priori. The topography should, on the one hand, be steep enough to narrow down the width over which the boundary current has to be observed thereby limiting the number of individual moorings, but on the other hand smooth enough to ensure a reliable planning and deployment of the individual moorings.

When the decision of the location of a boundary current meter array has been made, its extent toward the ocean interior, that is, its horizontal coverage, has to be addressed. Usually, the width of the Western Boundary Circulation System is not known precisely prior to the installation of the array and has to be estimated using other platforms. One attempt could be to perform a concomitant float experiment to estimate the horizontal boundary current structure (Fischer & Schott, 2002). The horizontal velocity structure of the boundary current can be obtained from binning drift velocities of floats, normal to selected depth contours (Fischer & Schott, 2002). Another method would be to rely on a high-resolution numerical simulation of the region (Hirschi et al., 2003). This requires thorough validation of the model performance against observations; otherwise, the model could guide the design of the mooring array to unsuited locations or spatial resolutions, leading to arbitrarily wrong results. Shipboard observations using ADCPs lowered with the CTD rosette (LADCP) and constrained with vessel mounted ADCP velocities deliver full depth sections of the velocity field, which can be used to estimate the boundary current width. However, one ship section provides only a snapshot and the flow field can be rather different in width and vertical structure during other times. Validating a numerical simulation with such ship sections might be a useful tool to estimate the best extent of the current meter array toward the ocean interior. A similar approach can be taken using satellite altimetry to investigate the best extent of an array. Another difficulty imposed on the horizontal mooring coverage are unanticipated recirculation cells as found at 53°N (Fischer et al., 2004) or 11°S (Schott et al., 2005). An incomplete resolution of such recirculation cells with a current meter array can introduce spurious variability to the resulting transport estimates of the flow, which needs to be evaluated (Hummels et al., 2015).

After deciding on the location and the extent of the array toward the ocean interior the different options of instrumentation and their vertical placement have to be considered. In general, for a baroclinic flow field observations, ADCPs or a number of single point meters (such as deployed near the western boundary at RAPID (Johns et al., 2008) and at 11°S (Hummels et al., 2015)) are required providing flow observations over an entire depth range. For barotropic flow regimes single point current meters can be sufficient. Upward looking ADCPs moored at a depth of several hundred meters are preferable to surface elements, when the chosen region is subject to strong fishing activity or ice drift, which can potentially lead to the loss of instrumentation moored close to the surface. However, fishing is not necessarily confined to the surface, and can also endanger instruments moored at or close to the seafloor (benthic fishing, e.g., bottom trawling). No general rule of thumb can be applied to ensure avoidance of bottom trawling. For examples, in the Rockall-Hatton area trawling can be as deep as 1,300 m, while, for example, north of Faroe Islands trawling seldom goes deeper than 500 m due to the hydrography in the area. Specific information on the intensity of fisheries in the area should be sought in advance of designing deployments. In general, ADCPs moored within a depth range of strong currents should be free of other instrumentation placed above, as a tilted mooring line will disturb the backscatter of the ADCP beams and induce errors due to wrong depth mapping of the measured signal. The recording of reliable tilt values is also necessary to transform velocities from beam coordinates to earth coordinates. In general, acoustic current meters perform well for the upper part of the ocean, where enough scattering particles and/or zooplankton is present. Within the deep ocean backscatter levels become low and mechanical current meters such as the Aanderaa rotor current meter (which are still used at, e.g., 53°N and 11°S), which are independent of particle abundance, might be the preferred choice. On the other hand, mechanical current meters stall when the velocity is only a few centimeters per second, yielding artificial observations of zero water speed, and thus might underestimate the mean velocity. Another point to consider when using ADCPs are unwanted interactions of the side lobes of the ADCPs with either the surface or a clean rock seafloor (Jochumsen et al., 2017). For some instrument types (e.g., the redesigned 75-kHz Long Ranger) ADCP side lobes may induce biases toward 0 on the velocity data if not properly accounted for (although this is not always the case).

When a current meter array has been successfully deployed and the data sets are recovered, the data have to be processed, correcting for magnetic deviation and mooring knockdown, and the observations of the individual instruments have to be gridded prior to estimating the transport of the boundary current flow. Usually, the individual velocity time series are low-pass-filtered (40 hr, thus detided), subsampled to, for example, 12-hr resolution and rotated such that the main flow component is along isobaths, which is generally parallel to the coast (Hummels et al., 2015; Zantopp et al., 2017). With processed observed velocity time series at hand a gridding method has to be selected in order to obtain a velocity field from which to calculate the transports. For some arrays such as 11°S the individual velocity observations are interpolated and extrapolated and a Gaussian weighted smoothing applied to obtain a full velocity field (Hummels et al., 2015; Schott et al., 2005; Zantopp et al., 2017). Another method is to perform a pattern regression analysis, where the patterns have to be obtained from high-resolution ship sections (Brandt et al., 2014). A prerequisite for the latter method is a sufficient amount of available ship sections, which is typically only the case when an array has been maintained over a longer period of time. A third method is to regress the observed velocity time series on a numerical model (Jochumsen et al., 2012), where again the model validation plays a crucial role. The fourth method listed here is based on multiplying vertically integrated measured velocities with a width associated to a certain current meter mooring assessed a priori during a period of full field observations (Beal et al., 2015; Jochumsen et al., 2017).

In a last step the velocity field obtained after data processing and gridding is integrated to derive transports between depth layers (Brandt et al., 2014) or density layers (Hummels et al., 2015; Zantopp et al., 2017). The latter studies use fixed density levels associated to certain water masses over an entire mooring period. For the Denmark Strait overflow, the upper boundary of the plume is assessed by finding the depth of maximum velocity shear (Jochumsen et al., 2017). Another approach is to use time varying boundaries for integration inferred from a time-varying density field. This requires the current meter array to be complemented with temperature and salinity loggers as done, for example, at Line W (Toole et al., 2011).

The strength of current meter arrays is their high temporal resolution of observations and their ability to observe the full flow field rather than just the geostrophic component. A weakness is that the spatial resolution both in the vertical as well as horizontally is limited for financial and operational reasons. Previously, instrument failure frequently led to huge data gaps in the time series introducing the difficulty of gap filling. While instrument performance has improved and total failures have become exceptional, data gaps due to mooring losses, funding issues or other unpredicted difficulties still occur in today's fieldwork. Current meter arrays are still rather cost intensive and therefore difficult to sustain over a long period of time.

3.4. Inverted Echo Sounders

As we have seen, for measuring transport time series across large spans (several hundreds to thousands of kilometers), the use of geostrophy is the most efficient and effective method. Inverted echo sounders equipped with a bottom pressure sensor (PIES) in combination with hydrographic profiles from Argo and shipboard CTD profiles provide a powerful tool to calculate continuous transport time series using the geostrophic method (Meinen & Watts, 1998, 2000; Mertens et al., 2009; Rhein et al., 2011). PIES moorings form the backbone of the SAMBA array measuring the AMOC at 34.5°S (Meinen et al., 2018; Meinen, Speich, et al., 2013). Furthermore, through comparisons when the PIES are deployed, altimetry can be used to extend the transport time series back to 1993, the start of the satellite altimetry (Roessler et al., 2015).

PIES measure the round-trip travel time of an acoustic signal sent by the PIES from the seafloor to the sea surface, as well as the bottom pressure. The acoustic round trip travel time, τ, can be derived as:

$$\tau = 2\int_0^p \frac{1}{\rho g c} dp, \tag{9}$$

where ρ is the density, c the sound speed, and p the hydrostatic pressure. In some oceanic regimes, each individual acoustic travel time is uniquely related to a density profile and to the associated specific volume anomaly (α). The calculation of the transfer function between τ and α is called the gravest empirical mode (GEM) technique (Meinen et al., 2000). Successful examples can be found for the Gulf Stream and the Kuroshio (Meinen et al., 2009; Mensah et al., Jan, 2016) for the subpolar North Atlantic (Rhein et al., 2011; Roessler et al., 2015) and other locations. Essential for the complete coverage of round-trip travel times from the PIES by the GEM transfer function is the availability of sufficient hydrographic profiles all year

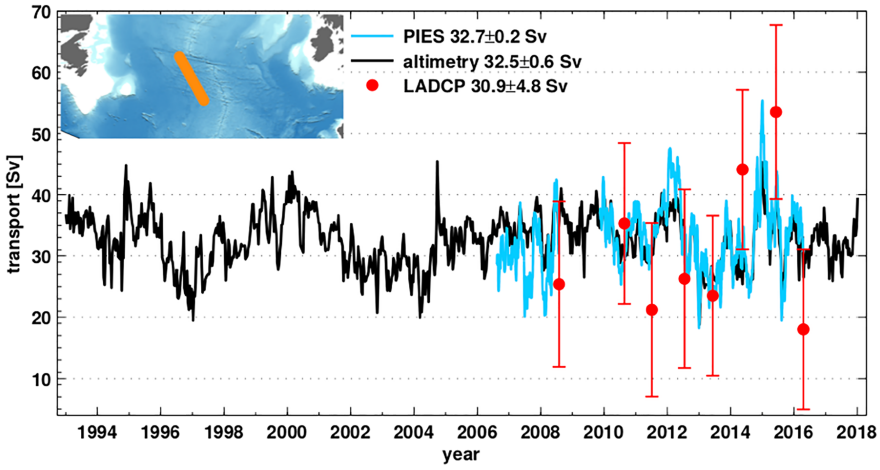

Figure 4. Bimonthly volume transport time series of the North Atlantic Current (from 47°40′N to 53°N) from the western into the eastern Atlantic relative to 3,400-m depth (update from Roessler et al., 2015). Blue: estimates based on the moored PIES. Black: based on the correlation between the altimeter surface velocity and the PIES transports. Red dots: transport estimates calculated from LADCP profiles taken along the PIES array. The vertical red lines denote the uncertainties. The mean of all three methods agree within their uncertainties.

round. In recent years, this is mainly due to the Argo program (Riser et al., 2016). More details on the calculation of the transfer function are summarized in Meinen and Watts (2000) and Roessler et al. (2015).

Once the transfer function is found, the dynamic height anomaly Φ at a PIES position is given by equation (7) with α inferred from the daily PIES measurements of τ. Having Φ determined at two PIES positions, the geostrophic velocity shear as well as the volume transport profile can be calculated via the geostrophic method as in equation (6).

As described in section 2, the geostrophic velocities obtained so far are relative to a chosen reference level. Although each PIES is equipped with a state-of-the-art pressure sensor, they all show unknown and different temporal drifts which have to be removed (Donohue et al., 2010; Watts & Kontoyiannas, 1990; Worthington et al., 2019) Once the drifts have been removed, the pressure differences between neighboring PIES reflect the barotropic transport variability, however they cannot provide the mean transport due to the well-known leveling problem (Donohue et al., 2010). On occasion, the absolute velocity at a reference level can be inferred from other available data (Meinen et al., 2000; Mensah et al., Jan, 2016). In other locations, geographic features provide obvious locations for assumed levels of no motion; for example, at the Mid Atlantic Ridge (Figure 4 updated from Roessler et al., 2015), the reference level can be chosen well below the ridge crest that blocks all flow, and so the reference velocity can be assumed to be 0.

At the PIES positions west of the Mid Atlantic Ridge at 47°N, the surface velocity inferred from satellite altimetry is highly correlated with the baroclinic transports as calculated from the PIES acoustic travel times time series (Roessler et al., 2015). By assuming that this correlation holds for the whole altimetry time series at these locations, the transport estimates from the PIES (deployed for the first time in 2006) were extrapolated back to 1993, the start of the altimetry measurements (Figure 4).

In the ocean interior, flows are in general broad and meandering so that to measure a transport, large distances have to be covered. PIES offer a very effective ways to do this, using the geostrophic approach. PIES can be deployed 3–4 years, and the data can be retrieved by acoustic telemetry. However, PIES measurements alone provide baroclinic and barotropic transport fluctuations, and the baroclinic time mean, but not the absolute transports.

4. Remote Sensing

Dedicated efforts to observe the AMOC require substantial resources. Therefore, there has been substantial interest in estimating the AMOC from existing sustained observations such as remotely sensed satellite data, in particular, satellite altimetry, and hydrographic data from autonomous platforms, in particular Argo data.

Satellite altimetry provides estimates of SSH above a reference ellipsoid (reference ellipsoid is defined as $z = 0$), which can be related to the dynamic height of the water column at the surface can be found by vertical integration of the hydrostatic equation (Williams et al., 2015):

$$\mathrm{SSH} + H = \int_{p_b}^{p_a} \frac{dp}{\rho g} \approx \frac{\Phi(p_a, p_b)}{g} + \frac{p_b}{g\rho_0}, \tag{10}$$

where $p(z = -H) = p_b$ is bottom pressure, $p(z = SSH) = p_a$ is atmospheric pressure at the sea surface, ρ_0 is a reference density, and $\Phi(p_a, p_b)$ is dynamic height at the surface of the ocean relative to the seafloor (as defined in equation (6)). Note that the motion of the seafloor and the impact of atmospheric pressure on SSH through the inverse barometer effect have been neglected. Often dynamic height fluctuations dominate circulation variability and the impact of bottom pressure can be neglected (Frajka-Williams, 2015). In those situations, SSH gives an estimator of surface flow and can be used as an estimator of dynamic height at any depth through the integral of $\frac{1}{g\rho}$. Satellite data has been quality controlled and combined from a number of satellite missions and is available from 1993 to the present.

The core Argo program (Riser et al., 2016) delivers profiles of temperature, salinity, and pressure from CTD sensors attached to over 3,000 autonomous profiling floats throughout the global oceans. The CTD data are delivered in both real-time and delayed-mode quality to global data acquisition centers and is freely available to users. Delayed-mode data go through a scientific quality control to correct for sensor drift (pressure and conductivity) if possible and delivers temperature, salinity, and pressure data to accuracies of 0.002 °C, 0.01 g/kg (or better), and 2.4 dbar (for delayed-mode data the estimated accuracies are provided in the data file). Typically, Argo floats perform a profile from 2,000 m to the surface every 10 days. Between profiling, the floats drift at a depth determined at deployment, most often near 1,000 m. This drift velocity can be used as an estimate of the 10-day absolute velocity at 1,000 m. Argo coverage is throughout the ice-free regions of the globe in water depths deeper than 1,000 m. However, coverage is reduced in the regions of swift-flowing or divergent ocean currents.

Multiple methods have been used to derive estimates of the transports associated with the AMOC from altimetry and remotely sensed hydrographic profiles. Mercier et al. (2015) integrated satellite altimetry with ship-based hydrographic profiles to produce a continuous time series and validate the ability of ship-based hydrography to capture interannual-to-decadal timescale variability. Willis (2010) took advantage of the relationship between profiles of the density anomaly (obtained from Argo float profiles) and SSH to derive monthly mapped fields of the density anomaly that are used to estimate the geostrophic shear at 41°N (equations (3) and (6)). The solution for the reference velocity, applied here as a barotropic adjustment, is based on deriving an estimated dynamic height at 1,000 m from the subsurface drift of Argo floats (Willis & Fu, 2008). Based on this approach, Willis (2010) reported that transport in the upper 1,130 m at 41°N varies between 9 and 20 Sv in 2002 to 2010. Using only altimeter data and the regression resulted in a similar range of values from 1993 to 2009 (8 to 20 Sv).

Following a similar approach to Willis (2010), Schmid (2014) constructed a three-dimensional geostrophic velocity field using temperature, salinity, and float trajectories from Argo and SSHs from AVISO. The relationship between dynamic height from Argo profiles and nearby daily SSH within 5° by 2° boxes with at least 10 data pairs are derived on a 0.5° by 0.5° grid and used to construct synthetic dynamic height fields. Monthly means of these fields are used to derive geostrophic velocity relative to a level of no motion at 1,000 dbar. Absolute geostrophic velocity fields are obtained using velocities estimated from the subsurface float trajectories following the method described in Schmid (2014). The hydrographic data from the profiling floats are also used to generate gridded fields of temperature and salinity in the upper 2,000 dbar, similar to the approach by Garzoli and Baringer (2007), Majumder et al. (2016) extended the velocity, temperature and salinity fields from 2,000 m to the seafloor by using World Ocean Atlas 2013 (Locarnini et al., 2013; Zweng et al., 2013).

The method used in Majumder et al. (2016) has been adapted to derive the AMOC transports at 26.5°N by taking the data from the Florida Current transport into account (following the approach used for the RAPID time series; for example, McCarthy, Smeed, et al., 2015). During 1993 to 2017, the resulting mean AMOC (Meridional Heat Transport) is 14.9 ± 4.4 Sv (1.10 ± 0.37 PW, Figure 5). During April 2004 to October 2015 the mean of 14.9 ± 4.8 Sv (1.04 ± 0.40 PW) is close to the 16.8 ± 4.4 Sv (1.08 ± 0.34 PW)

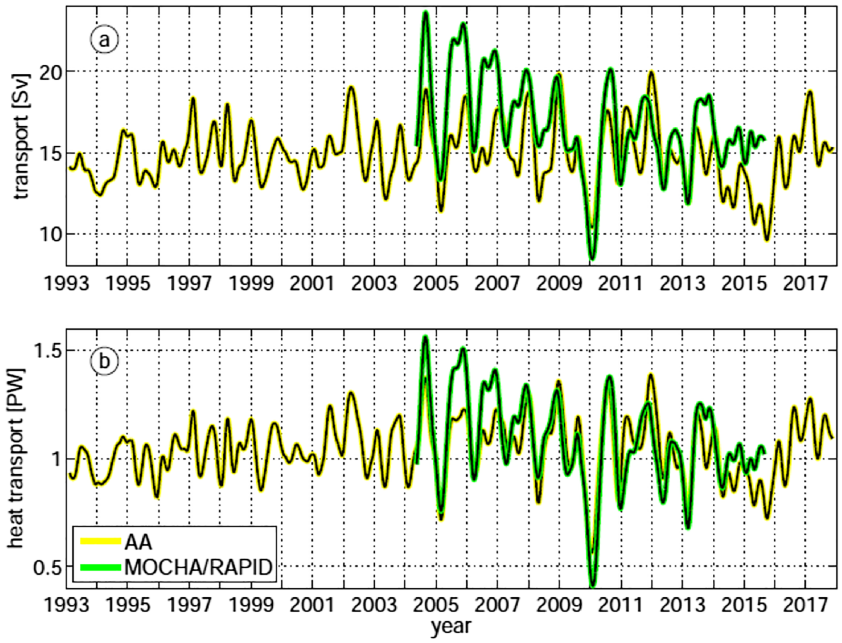

Figure 5. Three month low-pass-filtered transports at 26.5°N from synthetic dynamic height (AA) and MOCHA/RAPID (a) AMOC transport and (b) meridional heat transport.

from the RAPID mooring array, especially when the 1 Sv accuracy of the RAPID estimates are considered. Additional differences are likely due to the absence of deep data in the remotely sensed estimate. Both time series have a similar annual cycle, although the RAPID annual cycle is larger from 2004–2007, and a strong dropoff of the AMOC and Meridional Heat Transport in 2009/2010.

Similar blended satellite-in situ techniques have been tested, for example, Dong et al. (2015) derived synthetic temperature and salinity profiles by taking advantage of the relationship between SSH anomaly and the depth of given isotherms (e.g., Goni et al., 1996). The sea surface temperature for each synthetic profile was obtained from a gridded satellite-based product. Salinity profiles were generated using the synthetic temperature profiles and historical T/S relationships (Garzoli & Baringer, 2007). World Ocean Atlas 2013 was used in the deep ocean.

Frajka-Williams et al. (2015) used a simple linear regression between SSH anomalies in the west only, at 30°N and 70°W, to develop a proxy for the upper mid-ocean transport at the 26.5°N, which is the southward flow in the subtropical gyre above approximately 1,100 m. Following the RAPID methodology, the AMOC is estimated as the sum of the upper mid-ocean transport, the Florida Current transport, and surface Ekman transport. For the 1993–2003 period, the AMOC derived with this method has a mean and standard deviation of 18.3 $\pm$ 1.1 Sv, compared to the 2004–2014 period of 17.1 $\pm$ 1.7 Sv. The time series for the latter period shows the same major features as the RAPID time series, for example, Smeed et al. (2014).

Deriving synthetic temperature and salinity profiles rather than synthetic dynamic height profiles has the benefit of providing a better horizontal resolution of the temperature and density field used in the computation of the heat transport, for example. The advantage of relating the dynamic height (rather than temperature) to SSH is largest in the mixed layer where, as described above, the relationship between temperature and SSH breaks down. This can lead to a reduced accuracy of the geostrophic velocity derived from synthetic temperature and salinity profiles. Using SSH at a single fixed location at one latitude (and longitude) as a proxy for the upper mid-ocean transport at a different latitude is likely to result in larger uncertainties than the other two methods, because the coherence between the two latitudes could change over time. The weakness of all the methods using altimetry as a proxy is that they assume the relationship between SSH and the geostrophic velocity field does not change for the whole altimetry time series.

5. Additional Technologies

This section describes instruments and techniques that either contribute to one or no AMOC observing system but have the potential to.

5.1. ADCPs on VOSs

Much of our knowledge about the AMOC as a whole is derived from sporadic observations, such as shipboard hydrography (section 2), widely spaced observations, such as TMAs (section 3) or in combination remotely sensed data (section 4). Useful and vital as these measurements and techniques are, there is much they are unable to capture, including the most energetic part of the velocity spectrum, the structure of eddies and fronts, the deep velocity field and many circulation features in shallow seas and coastal areas. The ability to measure currents globally from vessels underway enables us to track what the ocean is doing in real time and markedly improve our predictive capabilities by enabling truly rigorous validation and verification of the interior dynamics of ocean circulation models. In this regard, commercial ships have a presence on the high seas second to none and offer society a feasible and cost-effective opportunity to contribute to solving this observational deficiency. And where commercial vessels are especially valuable is when they are assigned to the same track several times each month or each year for many years. Under these circumstances the growing data sets address the temporal as well as the spatial variability inherent in the ocean.

Over the past few decades the development of automated ship-based measurement systems has made great strides to that many of these systems can be deployed on ships without the constant attention of ship technicians. Included in this suite of sensors, the most common are ADCPs, thermosalinographs, pCO_2 systems, meteorological packages, ocean skin temperature radiometers, and automated XBT launchers. Of particular relevance for observing the AMOC are ADCP measurements.

Many of the ship-based observing systems were developed on research vessels, as was the case for ADCPs. A major advance for ADCPs has been the development of highly accurate heading information from either inertial and/or GPS-based systems. ADCP velocities are particularly sensitive to heading errors as, for example, when a ship steams at 5 knots, a 1° heading error results in cross-track velocity errors of 8.5 cm/s. As a result of improved heading, properly calibrated ADCP systems can now produce absolute velocity estimates approaching 1 cm/s accuracy. This level of accuracy allows ADCP data to be used to quantify upper ocean transports over long distances, which has proved to be an enormous asset when averaging out short temporal and spatial variability to illuminate the background velocity and transport structure.

While commercial vessels make the highly desirable repeat transects, it is neither practical nor desirable to send skill marine techs to watch over the equipment. Therefore, self-contained automated systems are needed. The first of these for ADCPs was AutoADCP developed for the container ship MV Oleander that runs between New Jersey and Bermuda (Flagg et al., 1998). AutoADCP had a number of useful attributes including the ability to monitor the ADCP to make sure it was operating and if not, restart the system. It also would shut down the data collection if the ship was in port or, in the case of cruise ships, to shut down the system when the ship slowed for a deep ocean swim. When AutoADCP was developed, the high cost of satellite communication precluded communication to shore except when in port. Thus, the ADCP data only became available at the end of a cruise. In recent years this situation has changed and many ships have satellite communication accessible either through the ship's or other dedicated network. This and other limitations with AutoADCP motivated the development of a more capable system based upon the University of Hawaii's UHDAS (University of Hawaii Data Acquisition Software, Firing, 1991). UHDAS is the system used on all the United States and many foreign research vessels. It is a robust system with a long track record. The UHDAS system was upgraded to incorporate some of the capabilities of the old AutoADCP but also offer the advantages of the UHDAS system such as daily call-ins giving the health of the system as well as providing partially processed data that can be telemetered ashore. This system is now running on two VOSs, the MV Oleander and MF Norrona, and is being ported over to several more.

At time of writing, seven commercial vessels equipped with ADCPs: the container vessels MV Oleander that operates between New Jersey and Bermuda, the MV Nuka Arctica that runs between Denmark and Greenland, and the MV Condor that operates along the coast of Chile, the high seas ferry MF Norröna out of the Faroe Islands that runs between Denmark and Iceland, and three cruise ships that operate out the U.S. East Coast and run between Bermuda, Miami, and the Caribbean, the MV Explorer of the Seas,

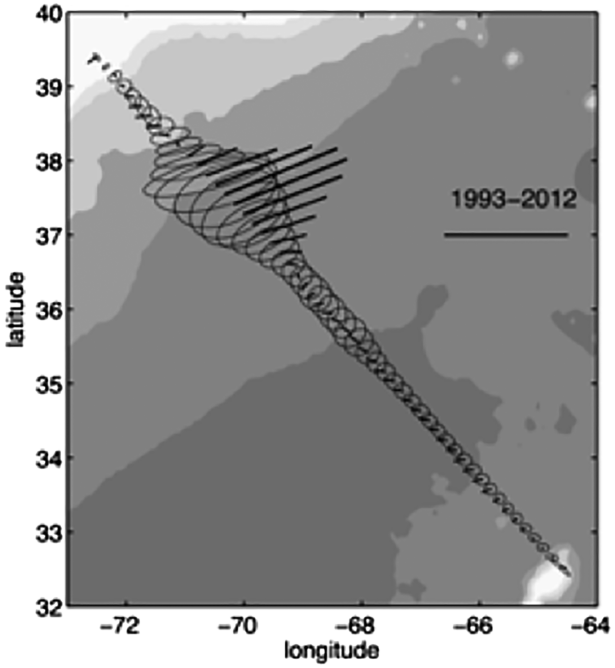

Figure 6. Mean velocity and variance ellipses between the mid-Atlantic Bight shelf break and Bermuda at 52/55 m depth from the MV Oleander for the 1993–2012 period. The bar corresponds to 1 m/s and 0.5 m^2/s^2, respectively.

MV Adventure of the Seas and soon, the MV Celebrity Flora. Discussions with international shipping organizations indicate that there is widespread support for VOS activities and our experience indicates a willingness by owners and crews to assist in these efforts. The existing VOS vessels support ADCPs operating at 150, 75, and 38 kHz with nominal ranges between 200 and 1,000 m. The cruise ship MV Adventure of the Seas and the replacement of the MV Oleander that is currently under construction, support two ADCPs, a higher frequency unit to survey near the surface and in shallow waters, and a lower frequency unit for deep water surveying.

An example is given below which illustrates the power of ADCPs on VOS ships. Figure 6, is a profile of the Eulerian mean and standard deviation velocities in the upper 50 m of the Gulf Stream from 20 years of data collected from the MV Oleander (Rossby et al., 2014). The Gulf Stream is characterized by a high degree of structural variability and large north-south migrations, of the order of 100 km, and obtaining a true mean picture of the transports requires many realizations to reduce the uncertainty to reasonable levels. The section means also resolve the westward mean flow in the slope sea, an area dominated by Gulf Stream meanders, warm core rings and shelf-break frontal eddies such that the noise level is extremely high. This level of spatial resolution of the mean field is only possible under conditions of repeated sampling such as that provided by the VOS fleet.

Yet another example of the utility of VOS comes from the combination of the Norröna and the Nuka Arctica where heat and salt fluxes are measured directly when ADCP data are combined with XBT and climatological salinity data (Rossby & Flagg, 2012). The accuracy of these estimates is governed by velocity uncertainty, not that of the temperature or salinity fields (although they are important). Ships in regular traffic scanning velocity have the potential to push the envelope in monitoring low-frequency variability of the AMOC and its associated fluxes.

5.2. Bottom Pressure

All proposed methods for monitoring the zonally integrated flows responsible for the AMOC involve the (generally good) assumption that the flow is predominantly geostrophic below the surface Ekman layer. Given this assumption, the most straightforward method to monitor the circulation in z coordinates would be to measure pressure differences between the eastern and western boundary at each depth. Model simulations show that this works well down to around 3,000 m, even with only western boundary measurements (Bingham & Hughes, 2008). Unfortunately, technology limits this method for two reasons. First, ocean BPRs suffer from instrumental drift which limits their capability on timescales comparable to a deployment length. Second, we cannot know precisely the depths at which the instruments are deployed (i.e., the well-known leveling problem; for example, Donohue et al., 2010). As a rule of thumb, if we are interested in an accuracy of about 1 Sv, then we need measurements at the level of 1 cm, or 1 mbar pressure (100 Pa).

There are, however, ways to get around these difficulties. The vertical sidewall ocean provides the template: here, as described in section 3.2, measurements of density at the boundaries allow for the calculation of from hydrostatic balance, which leaves only a single constant pressure to be determined at each time. This constant can then be calculated from mass balance (on the assumption that the net transport across the section is known, and must consist of the sum of known wind-driven Ekman transport plus the net geostrophic transport). The "sidewall pressure" is the relevant form of "bottom pressure" in this case.

In the absence of vertical sidewalls, two approaches are possible. The first, as described in section 3.2, is that taken by the RAPID array, in which density profiles are measured at two vertical moorings enclosing an "interior box" of the ocean, and currents are explicitly measured in the "triangles" between these moorings and the coast. The same argument as above is then applied, with the "triangle" flows added to the Ekman

flow to be balanced by the geostrophic flow in the "interior box." This method can also be thought of as a means to determine boundary (bottom) pressures, with the moorings used to calculate pressures at the boundaries of the "interior box," and current measurements used to extrapolate these to the boundary using geostrophy.

The second approach is the "stepping method" (Hughes et al., 2013), as used by the West Atlantic Variability Experiment (WAVE) on the RAPID-Scotian line near to Halifax. This uses only ocean bottom measurements to achieve the same end. In this method, the hydrostatic relationship (equation (5)) is generalized to apply to "sloping moorings", that is, a series of ocean-bottom instruments on the continental slope, in the form

$$p(z_c)-(z_a) = -\int_{z_a}^{z_c}\left(\rho g + \frac{\rho f u_L}{H_s}\right)dz, \tag{11}$$

where $p(z_c)$is the bottom pressure at $z = z_c$and $p(z_c)$is the bottom pressure at $z = z_a$, which is assumed to be shallower (i.e., the integral proceeds down the slope, such that dz is negative). Here, u_L is the horizontal velocity to the left of the (horizontal component of the) path of the integral, and H_s is the slope of the bottom (which will be positive as the bottom is at $z = -H$, and the depth H is increasing as horizontal distance increases). Equation (11) can be seen to approach equation (5) when the slope is very steep.

The reason for calling this the stepping method is because of its application with a finite number of instruments on the slope. For each pair of instruments, which measure near-bottom density and current, the current is used to determine the horizontal component of the pressure difference (assuming geostrophic balance), and the density is used (assuming hydrostatic balance) to determine the vertical component. This allows pressure differences to be integrated down the slope in the manner of a staircase.

Equation (11) shows that the vertical pressure gradient down the slope depends on density exactly as in hydrostatic balance for a vertical mooring, but also on the current, to an extent which depends on how steep the slope is; steeper slopes result in a weaker influence of the current term. The relevance of this can be seen by estimating how large a current is needed to produce a 1 mbar (100 Pa) pressure difference over 1-km depth range. This means that on a typical continental slope of gradient 0.05 (as seen in WAVE) significant pressure signals result from a current of only 5 cm/s. In contrast, the western boundary near the RAPID array (Rayner et al., 2011) has a very steep slope of over 0.5 over much of its depth range, leading to much weaker sensitivity to currents. The same is not true at the eastern boundary, which has a typical slope of 0.01 at this latitude.

Hughes et al. (2013) demonstrated that the stepping method measures pressure differences over a vertical downslope distance of 1,500 m, to an accuracy of better than 0.5 mbar (Figure 7). This error is comparable to that from the hydrostatic balance alone and was obtained in a region where the current variability dominates the integral (though density becomes more important at longer time scales, meaning closer to annual in this case). All that is required for this method is a series of short moorings measuring near-bottom currents and density just outside the bottom boundary layer (an ADCP mounted at 50 m above the bottom, and a MicroCAT temperature-conductivity-pressure recorder at 100 m were used in WAVE, with vertical downslope spacings of 500–600 m).

Unlike a direct bottom pressure record, the stepping method does not rely on data continuity to maintain the fidelity of a time series, since knowledge of instrument depths is only required to an accuracy of a few meters. It does, however, have the same limitation as the method, which relies on hydrostatic balance at tall moorings: The net geostrophic transport across the section must be determined by other means in order to provide the missing constant of integration. An alternative to this may be found by using a combination of satellite altimetry and a single tall mooring to determine bottom pressure at one depth. This method was investigated by Williams et al. (2015) and was found to be capable of determining the missing constant at an accuracy of 1–2 mbar (translating to midlatitude transports of 5–10 Sv over a 5-km-deep ocean). Such accuracy requires the most careful calibration and, particularly, high resolution in the upper few hundred meters extending into the surface mixed layer.

Although the stepping method obviates the need to use BPRs, with their drift problems, their use is still highly valuable as a check on the inferred pressure differences, and to fill gaps resulting from instrument failures. The drifts are usually very well characterized by an exponential plus linear trend (though

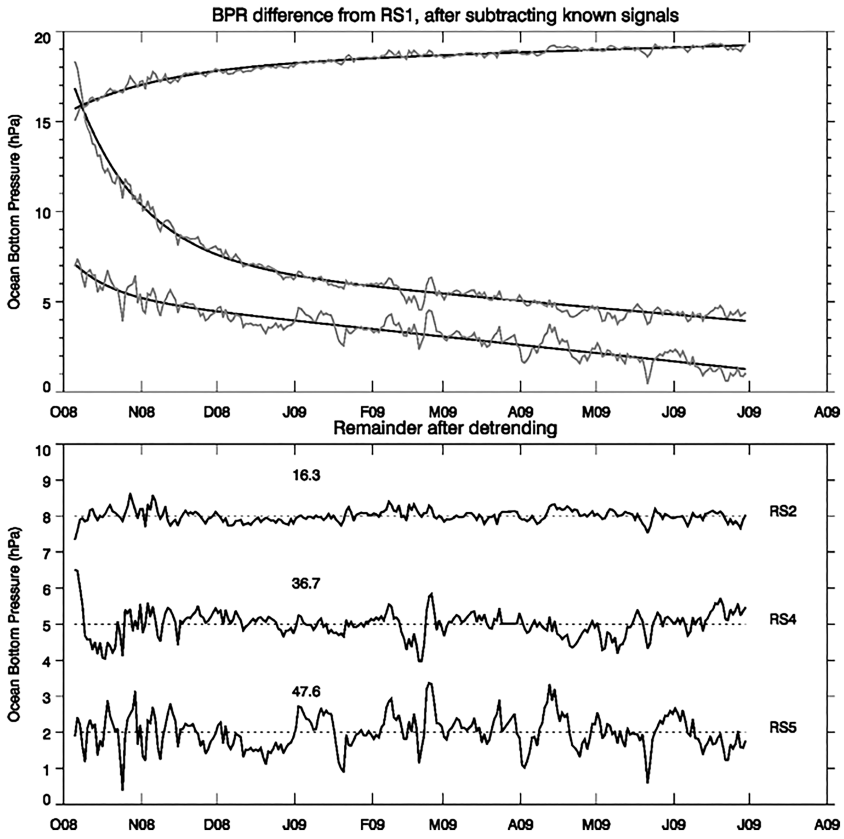

Figure 7. Comparison between directly measured bottom pressure differences and those inferred using the stepping method at the WAVE array (reproduced from Hughes et al., 2013). The difference as measured by BPR is shown, after subtracting the difference inferred from the stepping method. (top) Before detrending the BPR using the exponential plus linear fit shown. (bottom) After detrending. The differences are relative to mooring RS1 at 1,114-m depth. RS2, RS4, and RS5 are at 1,701, 2,784, and 3,427 m, respectively. Numbers in the bottom panel are standard deviations in pascals (1 mbar = 100 Pa).

different and with different time constant for each deployment). They also allow access to the part of the pressure field which does not vary with depth down the continental slope, permitting (at some frequencies) a direct test of the mass balance argument used to provide that missing constant more generally. In fact, Kanzow et al. (2007) confirmed that this works by using bottom pressure differences to calculate bottom geostrophic velocities, effectively using the formalism of equation (11) indirectly. Furthermore, there are hopes of obtaining better direct bottom pressure measurements in the future by improving measurement and calibration procedures (Worthington et al., 2019). A particularly promising development is the so-called 0-A-0 calibration procedure (Kajikawa & Kobata, 2014), which offers a means to reduce instrumental drift, and has shown very promising initial results.

Thinking in terms of bottom pressure also clarifies a number of issues about the effectiveness of AMOC monitoring systems. As pointed out by Wunsch (2008), the ubiquity of energetic eddy fluctuations in the ocean means that a measurement of transport integrated between two typical points tends to be dominated by mesoscale variability at those end points, meaning it does not reflect the large-scale ocean circulation in a meaningful way.

This argument is valid when one of those end points is in the open ocean. However, it fails when the integral is right across the ocean, because the measurement at the end points is then of bottom pressure, and mesoscale eddies have little influence on bottom pressure on a steep continental slope. In a model context, this was demonstrated by Hughes et al. (2018), who showed that bottom pressures on the continental slope do reflect large-scale dynamics and the AMOC very clearly and that the model variability is consistent with satellite sea level measurements and bottom pressures in the WAVE array. Hughes et al. (2018) explain this with a

simple scaling argument, based on the inability of vorticity balance to produce large vertical velocities. The suppression of mesoscale energy at the boundary was also observed and justified in a vertical sidewall context, by Kanzow et al. (2009).

Returning to the AMOC, as the continental slope becomes gentler at depth, the suppression of the mesoscale variability relaxes, and strong bottom pressure variability is seen again, particularly in the western basin. This, together with insufficient bottom current measurements, may help to explain a discrepancy at the RAPID array between monitoring the zonal-and-depth-integrated flow below 3,800 m in the model simulations of Sinha et al. (2018), despite working well for shallower flows. Monitoring these deeper flows is much more challenging, mainly because the "sidewalls" are much less steep, a factor which also adds to the role of any ageostrophic bottom Ekman flow.

Finally, on the subject of ocean bottom pressure, we should consider the capability of satellite gravity measurements from GRACE and subsequent missions. Landerer et al. (2015) showed promising agreement between GRACE-derived estimates of the lower branch of the AMOC, and those from the RAPID array at 26°N, obtained by differencing satellite-derived bottom pressures averaged over the eastern and western continental slopes between 3,000- and 5,000-m depths. While this is very interesting, there are reasons to be skeptical about the general validity of this technique. The GRACE measurements used are averaged over 3° spherical caps, which is wider than the continental slope in most places. They thus rely on the extension of the bottom pressure signals beyond the continental slope in order to be able to resolve the signal (GRACE certainly does not have the resolution to distinguish between the upper and lower continental slope). However, a variety of model simulations (Bingham & Hughes, 2009; Roussenov et al., 2008) show the relevant pressure signal to be tightly confined to a narrow slope region, and local wind stresses are responsible for a major part of the variability observed on the continental shelf (Piecuch et al., 2016). We must therefore ask whether the ocean is behaving differently from the models, or whether the match is at least partly coincidental. It is possible that the averaging effect of GRACE is working to our advantage. One possibility is that the deep signal is indeed coherent with the lower slope on large scales but is locally masked by mesoscale variability which is filtered out in the GRACE data. Another possibility is that the particularly large AMOC signal in 2010, associated with highly unusual winds, reflects an atypical and predominantly barotropic response with broader length scales than usual.

For the present, satellite gravity must be considered an unproven means of monitoring the AMOC for the present. However, the results are intriguing and more investigation is certainly worthwhile.

5.3. Cable Measurements

Another technology being utilized for AMOC-related observations involves voltage measurements on an ocean-bottom out-of-service telecommunications cable across the Florida Straits (Meinen et al., 2010). Basic electromagnetic physics indicates that charged particles moving through a magnetic field cause an electric field perpendicular to the motion—in practice for physical oceanographic purposes this means that flows of seawater (carrying salt ions, i.e., charged particles) moving through the Earth's magnetic field can create horizontal electric fields that are proportional in strength to the amount of seawater being carried (Larsen, 1992; Larsen & Sanford, 1985; Szuts, 2012). The actual application of this basic physics to oceanographic measurement is complex, and specifically, it is complicated by two factors that make implementation difficult. First, the calibration of the cable voltage-derived transports must be routinely monitored by independent ocean velocity/transport measurements such as ship sections, which can be time and resource intensive. Second, a portion of the induced electric field can "short out" through ocean sediments, and the impacts on the electric field are different for different sediment types. As a result of the latter issue, if a constant oceanic flow meanders over different types of sediments, the induced electric field strength will vary even though the transport of the ocean flow is steady. Both of these issues limit the application of this cable-voltage technique greatly.

One location where the method has been shown to work well is in the Florida Straits at 27°N, where the Gulf Stream (the Florida Current) is routinely observed by ship sections and where the flow fills the Straits, and as such it cannot meander over different sediments. Voltage measurements on a cable that spans the Straits at this location have yielded daily estimates of the total integrated Gulf Stream/Florida Current volume transport almost continuously since 1982 (Larsen & Sanford, 1985; Meinen et al., 2010). Numerous (100+) ship

sections making direct ocean velocity observations near the cable site have been collected and used to monitor and correct the volume transport calibration of the cable over the past 30+ years, as well as to develop parallel calibrations to estimate both temperature and salinity transport from the cable voltages (Garcia & Meinen, 2014; Shoosmith et al., 2005; Szuts & Meinen, 2017).

The daily Gulf Stream/Florida Current volume transport time series at 27°N has been a key component of the basinwide AMOC volume transport estimates at 26.5°N made by the RAPID array since the array was first deployed (Cunningham et al., 2007; McCarthy, Gleeson, & Walsh, 2015). The high-temporal resolution cable measurement system has been reliable for many years, depending on the availability of submarine cables and the goodwill of the telecommunications companies that operate them (Batelco and AT&T). The Gulf Stream/Florida Current observing system is envisioned as continuing forward indefinitely based on modest support from the National Oceanic and Atmospheric Administration Western Boundary Time Series project—the only "end" of this observing project would be due to elimination of National Oceanic and Atmospheric Administration funding or the breaking of the submarine cable itself.

Implementation of cable-voltage ocean-transport measurement systems in other locations is being explored (Nilson et al., 2007; Sigray et al., 2004); however, the difficulties of routine calibration monitoring and meandering over different sediments are significant, and further application to AMOC monitoring has yet to be implemented.

Cabled observatories have become a feature of ocean observing, particularly led from North America, predominantly as a form of data telemetry (see section 6.2.1). However, it has been proposed that the instrumentation of telecommunications cables could provide bottom temperature and pressure data that could be used of AMOC observing (Howe et al., 2019). This is as yet unproven but a potential future development of cable observations as part of AMOC observing systems.

5.4. Gliders

Gliders are autonomous vehicles which move vertically by changing their buoyancy and move horizontally due to the lift provided by their wings. They complement other in situ observing platforms (research vessels, Argo floats, drifters, and mooring arrays) by covering scales from 1,000 km down to the microscale, and timescales from years to minutes (Liblik et al., 2016). Over the last decade, gliders have been especially useful in observing (i) the coastal/open ocean transition zone, (ii) ocean's boundary currents, (iii) water mass transformation regions, (iv) polar regions, (v) mesoscale and submesoscale structures, (vi) internal wave and turbulence, and (vii) biological/biogeochemical processes (Liblik et al., 2016; Rudnick, 2016; Send et al., 2010). Since 2014, underwater gliders are used routinely as a component of trans-oceanic AMOC observing system, OSNAP, to monitor the NAC (Houpert et al., 2018; Lozier et al., 2017).

Gliders move vertically in the water column by changing their buoyancy and achieve vertical speeds of 10–20 cm/s. Thanks to their wings and their pitch controlled by movable internal battery packs, gliders follow sawtooth paths through the water, moving with a typical horizontal speed of 20–30 cm/s. Either by controlling their roll or by moveable rudder, horizontal direction can be controlled. Standard gliders can profile from the surface to 1,000 m, and recently, deep glider models can profile up to 6,000 m over a year. When profiling to 1,000 m, a dive cycle takes about 4–6 hr and the glider travels about 4–6 km. The relatively low energy needed by buoyancy-driven gliders make them suitable for long-endurance missions lasting several months and covering thousands of kilometers.

Over each dive cycle, the depth-averaged current (DAC) can be calculated by differencing the horizontal displacement estimated from a hydrodynamic model from the actual glider displacement derived from GPS positions (Eriksen et al., 2001; Rudnick & Cole, 2011). The DAC accuracy is within 1 cm/s for a glider with stable flight characteristics (Eriksen et al., 2001; Todd et al., 2011).

Using the DAC, gliders estimate reference velocity (equation (4)) and hence absolute geostrophic velocity, using equation (7) between two successive profiles. These can be used to quantify boundary current transports.

When referencing the geostrophic velocity to the DAC, it is assumed that the DAC is essentially geostrophic. This implied that the glider has to dive deep enough in order for the surface Ekman current to have a negligible contribution to the DAC, and the contribution of tidal current has to be removed if the glider is

operating in a tidal-dominated environment. A possible alternative is to perform direct measures of absolute velocity profiles by integrating ADCPs to the glider (Todd et al., 2017).

The growing maturity of glider technology and community led to the recent recognition of the OceanGliders program by the WMO-IOC Joint Technical Commission for Oceanography and Marine Meteorology, as a component of the Global Ocean Observing System. In complement with other existing observing networks, the scope of sustained global-scale glider activities is therefore defined and promoted in key regions of the ocean, particularly relevant for AMOC monitoring.

The strengths of using gliders in an AMOC monitoring system are (1) the real-time data (every 4–6 hr the glider transmit temperature-salinity profiles and DAC); (2) the high spatial resolution (two dive cycles are separated by 2 to 6 km); (3) measurements up to the surface; (4) estimation of absolute geostrophic current (the DAC is directly estimated by the glider and used as a reference); and (5) measurements of biogeochemical variables (additional optical sensors are routinely integrated to gliders, such as oxygen).

The weaknesses are essentially (1) their low temporal resolution compared to mooring (with 8 to 24 km traveled per day, a glider need between 4 and 12 days to travel 100 km); and (2) the heavy logistic involved in maintaining an endurance line; for example, four glider missions per year will need at least a part-time technician to execute program and additional human support for the piloting and the deployment/recovery operations. In order to aim for a 100% good data return, it is also necessary to plan for a "backup" glider on standby and ready-to-go at all times, in case of instrument failure (Brito et al., 2014).

These strengths and weaknesses make gliders particularly relevant for boundary current monitoring: Boundary currents are located close to the continental slope and their typical scales are of the order of 50 km. In addition, glider can also be operated to continuously monitor a specific location, providing data that resemble a virtual mooring/profiler. In the context of a basinwide mooring array transmitting real-time data, this configuration could be considered as an emergency solution in case of a lost/failure of a key-mooring for the basinwide AMOC transport calculation.

6. Observational Gaps

6.1. Geographical Gaps

6.1.1. The Continental Shelf

Paradoxically, it is their shallow nature that allows the influence of the shelf seas to imprint deeply on the world's oceans. The abyssal ocean is filled with waters transformed by buoyancy loss to the atmosphere, and it is in the shallow seas that buoyancy loss can create the heaviest water. Particularly, the deep cell of the AMOC, fueled by AABW formation in the Weddell Sea, but also in the northern limb of the primary cell near the northern European continental shelf and the Arctic shelf sea where dense water cascades from the shelves and into the abyss. These dramatic diabatic transformations in shelf seas are augmented by adiabatic transformations, again amplified by the topography of continental shelves: strong tides in shallow seas and strong currents associated with steep continental boundaries. Without water mass transformation, there is no AMOC, and arguably, our understanding of the processes of water mass transformation, their distribution, and their magnitude lag considerably our understanding of deep ocean circulation. AMOC sensitivity to freshwater buoyancy input has been demonstrated in a number of studies (Rennermalm et al., 2007). Of all the world's fresh water, less than a tenth of 1% is held in the atmosphere; it resides as ice (~70%) or groundwater (~30%) and so enters the ocean via rivers or tidewater glaciers, both continental features. Finally, middle- and low-latitude Mediterranean seas, though sometimes of great depth and perhaps not always considered as continental shelf seas, may experience considerable evaporative densification, communicating this with the adjacent Atlantic Ocean as strongly modified water masses spreading at intermediate depth.

In these ways the continental shelves have relevance to the processes of the AMOC. Observing these processes at the continental boundaries (e.g., intensified boundary currents and the "triangle" problems in geostrophic estimations) has been covered elsewhere (sections 2 and 3), but observing on the shallow and/or seasonally ice-covered continental margins offers some unique observational opportunities (due to the proximity of land) and challenges (due to ice, exceptional currents and fishing).

There are many motivations to observe continental shelves, beyond interests in AMOC: fisheries, aquaculture, oil and gas extraction, off-shore energy, transport, tourism. And often, it is this breadth of

motivations that lead to observing systems not necessarily designed for a single purpose and rarely for considering the impact shelf processes on the AMOC. A diverse range of interests and stakeholders also guarantees rapidly changing and evolving shelf observing systems. We therefore comment only on observing systems that specifically relate to the North Atlantic and confine other comments to generalities and principles of coastal and shelf observing systems. For more details of present observing systems and greater detail on the generalities we point the reader toward (Brink & Kirincich, 2017).

Continental margins surrounding the Atlantic comprise the narrow coastal strip of much of West Africa and northern Brazil, the wide margins of Patagonia, New England, from NW Europe across the GSR to north America, and the extensive high-latitude seas of the Weddell Sea in the south to Barents and Kara Seas in the north. In context of AMOC, narrow margins are arguably of lesser interest or accessible by techniques already covered in earlier sections. We note also GO-SHIP reference lines, all of which cross continental shelves, though often with insufficient spatial resolution to resolve boundary current structure. Nevertheless, these sections provide limited synoptic views of the continental shelves. AMOC mooring arrays of RAPID and SAMBA have little presence on continental shelves. The OSNAP array does monitor the eastern boundary current of the subpolar gyre with a single conventional current meter mooring, but not the continental shelf. NOAC likewise currently stops before the continental slope southwest of Ireland. On the western boundary on the southeast Greenland and Labrador shelves OSNAP has conventional mooring arrays, but significant sustained maintenance difficulties due to fishing activity are experienced, and substantial data gaps exist. Indeed, both SAMBA and OSNAP use model data to augment the transport on the westernmost shelves, highlighting that the transport on the shelf is important but an observational gap.

The northwest European continental shelf does not have a coordinated observing system. Despite decades of EU framework programs and the long maritime histories of the Spanish, Portuguese, French, and British Empires, coordinated systems, such as those along the U.S. eastern seaboard, simply do not exist. There are, however, coherent European enterprises that combine national and subnational marine data and model output over the shelf seas. Most notably EMODnet for marine observations and the Copernicus systems for satellite earth observation and numerical model hindcasts and forecasts. Though there are some web navigational complexities, all these aspects have been brought together under the Copernicus Marine Environmental Monitoring Service (CMEMS), providing "regular and systematic core reference information on the state of the physical oceans and regional seas."

Generally speaking, the strategy developed in Europe has not embraced cabled observatories and invested in favor of Marine Autonomous Systems for sustainable continental shelf observation. Coordinated efforts to bring Ocean Gliders in the Global Ocean Observing System (GOOS) are underway via EuroGOOS, with a white paper written highlighting the special role of ocean gliders can play in the GOOS, including boundary currents associated with continental margins (Liblik et al., 2016). It is perhaps with the inclusion of ocean gliders into GOOS that greatest progress will be made with sustained observations of the extensive NW European shelf seas.

A notable exception to the paucity of sustained continental shelf monitoring of relevance to the AMOC (in addition to OSNAP) is the mooring array between Scotland and the Faroes, jointly maintained by these two subnational states (Hansen & Østerhus, 2000). An improved methodology for both these exceptions, by integrating ocean gliders and/or autonomous surface vehicles with trawl-proof acoustic current meters, is under evaluation.

Scientific relevance of the NW European shelf seas system to the AMOC are perhaps best reflected in two recent papers: one highlighting large localized inflow of an eastern boundary current onto the shallow continental shelf at 56°N (Porter et al., 2018) and a second predicting the possibility of large future decreases in the exchange between the North Atlantic subpolar gyre and the northern North Sea (Holt et al., 2018).

Freshwater export from the Arctic is greatest through the Fram Strait concentrated on the East Greenland continental shelf (Haine et al., 2015). Predicted future increases in both Arctic storage and export of freshwater to the North Atlantic have been shown in numerous studies to weaken the AMOC. Sustained observations on the southeast and southwest Greenland shelves are conventional mooring-based systems and currently undertaken under the auspices of OSNAP (Lozier et al., 2017). The wide Labrador Shelf, however, is lacking in sustained observations. Challenges to conventional moorings in these locations come from

Table 1
Commonly Used Observing Techniques in Coastal and Shelf Seas Observatories

Method	Platform	Spatial coverage	Temporal coverage	Typical applications
Drifters	discrete, drogued, mobile	10 to 1,000 km	Days to months	Circulation pathways, dispersion
Fluorescent tracers	Single point release from vessel, shore/river release	10 m to 50 km	Hours to weeks	Horizontal and vertical dispersion
HF radar	Land-based TX/RX stations	200 km	Continuous	Surface currents, harbors, narrows, headlands
Ferry boxes	Vessels of opportunity	Dependent on route	Daily to monthly	Interisland routes, passages
Wave systems	Fixed surface buoy moorings, subsurface acoustic moored	Single point	continuous	Model assimilation, safety at sea
Met buoys	Fixed moored surface	Single point	continuous	Model assimilation, safety at sea
Tide gauges	Shore based	Single point	continuous	Mean sea level, storm surges
Moorings	fixed	Single point	Continuous	various
Gliders	Mobile, directed	5 to >200 km (full shelf)	days to months	Frontal systems, boundary currents, storm/hurricane studies
AUVs	Mobile, directed	1 to 100 km	Hours	Coastal discharges, bed mapping/searching, inspection
ASVs	Mobile, directed	1 to 500 km	Hours to weeks	Mapping, routine inspection, shallow water hydrography

Note. AUV = autonomous underwater vehicle; ASV = autonomous surface vehicle.

fishing, ice, and particularly icebergs, and knock-down (an issue with estimating surface intensified freshwater transports). Ocean gliders have been deployed in SE Greenland and offer at present time a part solution. If overall reliability and ice-avoidance techniques can both be improved, as seem likely, a combination of bottom mounted acoustic profiling current meters and ocean gliders offers a promising solution to sustained observing of freshwater export from the Arctic into the Atlantic.

In the previous paragraphs, we identified the apparent strengths of combining conventional and new autonomous technologies for sustained observations on continental shelves, with reference to improved AMOC understanding. Specifically, the combined power of seabed-confined acoustic instruments with autonomous systems, for example, combining ocean gliders or autonomous surface vehicles with moored ADCPs or inverted echo sounders. The growing global reach of gliders for sustained ocean margin observing now has a clear roadmap explained in the white paper of Testor et al. (2019).

A tabulated list of commonly used technologies for observing continental shelves is shown in Table 1. More details of these methods can be found in many references, and we point the reader to Brink and Kirincich (2017) and references therein for an informed and thorough exposition. Two overarching themes are apparent in coastal and shelf sustained observing: (1) complexities of territorial water management, discontinuity and/or disconnected efforts, lack of coordinated historical archiving, changing priorities for coastal waters, and all present challenges to data discovery of existing shelf seas observation, let alone creating of new sustained observing programs; (2) the shorter time and space scales of variability in shallow continental shelf waters and the proximity to land favor the adoption of robotic technologies (gliders, autonomous underwater, and surface vehicles) and land-based methods (e.g., tide gauges and high frequency radar).

6.1.2. The Deep

Both overturning cells of the AMOC are defined by deep flows. The lower branch of NADW reaches to deeper than 3,000 m in the subtropical North Atlantic and all of the South Atlantic and AABW fills the deepest ocean basins below 5,000 m. Observations of these deep ocean flows face unique challenges. Typically, the deep oceans have a depth between 3,000 and 6,000 m and have a large breadth, for example, the Atlantic Ocean is 3,000–6,000 km wide. These topographical settings impose huge challenges in where and how to measure the deep flows. Many of these deep flows are very weak with weak stratification, which adds a restriction on the types of observations that are useful compared to observations of much stronger surface flows. The deep oceans are waters with low backscattering particle density, and this means that instruments such as ADCPs and other acoustic current meters suffer from low signal-to-noise ratios (Hogg & Frye, 2007). Instruments have to withstand the extremely high pressure at these depths. To withstand the pressure, titanium housings are needed and electronic parts as well as battery endurance have to be able to withstand the persistent low temperature conditions in the deep ocean. Furthermore, all other mooring parts, such as

buoyancy and releases, must also be suitable for this extreme environment raising the costs of instruments suitable for deep water observations.

Deep near bottom current cores often are not aligned with structures in the water column above, leading to baroclinic velocity profiles and the need for more moorings when basin wide sections are to be covered (e.g., the overflow core in the DWBC, see Zantopp et al., 2017). Abyssal flows away from the western boundary are generally slow and broad, when they are not confined by channels in the bordering ridge systems. Geostrophic approaches can be used, but results depend on the choice of zero velocity (Johnson et al., 1994). The accuracy of the hydrographic data must be high; otherwise, gradients within the weak stratification of the deep ocean will not be resolved sufficiently. Furthermore, common mapping procedures used for the production of gridded data needed for transport calculations generate information only to the deepest common level of mooring pairs. Especially at rising topography near the boundaries large areas of no information remain near the bottom, which have to be filled by extrapolation.

Abyssal water masses gain buoyancy by either geothermal heating or diapycnal mixing with less dense water from shallower levels, forcing the bottom waters to slowly upwell. This is a necessary process to close the global ocean circulation. However, the locations of significant vertical motions are not well constrained so far, although water mass modification due to mixing is apparently linked to rough topography and channels (Voet et al., 2015). The number of canyons in ridge systems has been estimated to be in the order of 10^4 (Thurnherr et al., 2005), and hitherto, only few of them have been sampled leaving a huge observational gap.

In more recent years a variety of floats and gliders have been developed with one of the aims being to reduce expensive ship time. Again, most of these instruments have a depth limit of 1–2,000 m and are thus not suitable for the deep abyssal leaving it unobserved. For instance, in the Argo program almost 4,000 floats are constantly observing the upper 2,000 m of the world oceans, while only around 50 deep Argo floats that observe depths greater than 2,000 m are in operation. This also highlights the importance of the oceanographic research fleet—maintaining the necessary mooring arrays and/or ship sections in the deep will continue to require research vessels capable of working in these regions.

The main challenges in observing the deep ocean flows thus are the vast area that these flows occupy and the huge costs of special instrumentation and extended ship time that are needed to provide reliable observations. Nevertheless, the continuous development of new measurement techniques and cheaper and smarter instruments constantly improves the opportunities to obtain additional observations in the deep ocean at a lower cost.

6.2. Parametric Gaps

6.2.1. Real-Time Data

The timely return of oceanographic data is increasingly important for assimilation in computer models. The real-time return of meteorological data has long been important for initialization of weather predictions, and there are many land-based and coastal mooring sites that transmit parameters such as wind speed, direction, humidity, and air temperature. Similarly, there are many shallow water tide gauges, current meters, wave measuring devices, and other instrumentation that return data for the control of shipping and water quality monitoring, and data from free-drifting floats provide data from some of the deep ocean but data from fixed locations, in particular, in the context of this paper, TMAs with no surface expression, are more difficult to relay to shore. Making use of these data can often be delayed with recovery of the self-logging instruments often being over a year or more after their deployment.

There are many other advantages to transmitting oceanographic data in real-time or delayed mode including: data security, which is important if instrumentation may be lost before recovery; prolonging deployment duration (and hence a potential financial saving) is enabled by telemetry as telemetry shows that the mooring is working; and, if two-way communications exist, allowing changes to sampling plans in response to changing in situ parameters.

Broadly speaking, sites where telemetry from fixed point moorings is required can be classed into geographic regions related to water depth and the proximity to land. Coastal sites are often in range of cellular phone networks or radio transmitters, but further offshore requires the use of extensive cable infrastructure (e.g., Neptune Canada, (Barnes, 2007), and the Ocean Observing Initiative Cabled Continental Margin and Axial Seamount Arrays, (Kelley et al., 2014)) or satellite communications. Deep water sites (water depth >

Table 2
Benefits and Weaknesses of Technology to Transmit Data Through the Water Column

Through-water data transfer method	Advantages	Disadvantages
Electrical cable	High data rate Can transfer power	Limited vertical range (<1,000 m) Multiple wires or expensive mooring wire
Acoustic	Good range (up to 6 km or more)	Low data rate High power requirement Possible noise interference
Radio frequency	Low power	Very short range (<5 m)
Light	High transfer rate	Need good alignment Need clear water Limited range (<300 m)
Inductive	Low power Good range (>6,000 m)	Low data rate Mooring design challenge

2,000 m), either close to or far from land, are most important for projects involved in collecting moored data for AMOC observing.

The method of using satellite communications can be divided further into those systems that have a permanent surface expression in the form of a buoy (e.g., the TAO (Tropical Atmosphere Ocean) array, (McPhaden et al., 2010), the PAP Observatory); those that have an intermittent surface expression such as a winched float (e.g., SeaCycler at Labrador Sea VITALs mooring site); and those that do not have a surface expression attached to the mooring but make use of releasable data pods (e.g., the U.S. Atlantic Oceanographic and Meteorological Laboratory's ABIISS, the U.K. National Oceanography Centre's MYRTLE, the German Develogic system, and the University of Rhode Island's system, and the Swedish KTH Royal Institute of Technology's LoTUS buoy) or relays through gliders or surface vehicles (Wave gliders and ships via acoustics).

Those deep water sites with a surface float tend to only instrument a part of the water column on a single mooring due to the challenges of both maintaining a mooring in the dynamic wave environment and providing a way of transferring data through the water column. There are several different techniques employed for data transmission within the water, each with their own relative merits (see Table 2), and those more commonly used for oceanographic moorings are inductive telemetry along the mooring itself and acoustic telemetry when sending data to another nearby mooring or data relay vehicle.

Successful deployments of such technologies in AMOC dedicated TMAs include across the GSR (Hansen et al., 2015) and successful trials involving the Myrtle X lander and Wave glider at the RAPID array.

6.2.2. Biogeochemical Measurements

The Atlantic Ocean plays a key role within the global carbon cycle, not only through its large net uptake of natural and anthropogenic carbon dioxide (CO_2) from the atmosphere but also its subsequent transport to depth on climatically important timescales (Broecker & Peng, 1992). CO_2 uptake occurs when surface waters become undersaturated with respect to the atmosphere, and the overturning circulation is a critical component of this phenomenon occurring; heat loss associated with the cooling of northward flowing warm waters increases seawater's solubility to CO_2 (Watson et al., 1995) while intense biological activity (sustained by the northward transport of nutrients from the Southern Ocean (Sarmiento et al., 2004) leads to substantial carbon drawdown (Sanders et al., 2014). Large-scale circulation variability has been found to strongly influence carbon dynamics, both through the upwelling of old waters high in remineralized carbon, and the sinking of surface waters with high loadings of human-derived CO_2 (DeVries et al., 2017). Within the Atlantic, circulation has been directly linked to impact sea surface carbon fluxes (Pérez et al., 2013).

There is thus clearly a need to monitor the behavior of the ocean circulation with respect to biogeochemistry and the carbon cycle, given its importance to the continued mitigation of atmospheric CO_2 levels and supply of nutrients to key ecosystems. Historically, the monitoring of the transport of biogeochemical parameters by the AMOC has been limited to opportunistic hydrographic sections or decadal transoceanic basin repeat sections conducted as part of global observing system initiatives such as WOCE, CLIVAR, and GO-SHIP (e.g., South Atlantic carbon transport (Holfort et al., 1998); North Atlantic carbon transports (Macdonald et al.,

2003; Pérez et al., 2013)). Recently, the French lead GEOVIDE cruise (Sarthou et al., 2018) have laid the foundations for geochemistry on the repeat OVIDE line sections (section 2). Higher frequency observations of changes in seawater chemistry have been limited to time series stations such as at Bermuda (BATS), the Canaries (ESTOC), the Iceland and Irminger Seas, and the Cariaco basin (CARIACO). This is because climate-relevant biogeochemical research requires high standards of measurement accuracy and precision that has hitherto restricted investigations to the laboratory as the development of technologies for the remote measurement of biogeochemical parameters has typically lagged behind that for physical parameters.

In the last decade, however, novel biogeochemical sensors and autonomous samplers have begun to overcome the substantial technical difficulties that have restricted their application from remote environments. Optical fluorescence-based optodes for dissolved oxygen have become an integral addition to profiling floats (Bushinsky et al., 2017; Körtzinger et al., 2004), while sensors for nitrate (based on ultraviolet spectrophotometry, e.g., Johnson et al., 2017), pH (based on ion sensitive field effect transistors technologies, e.g., Martz et al., 2010; Bresnahan et al., 2014 or spectrophotometry, e.g., Cullison Gray et al., 2011 and pCO_2 (based on infrared/colorimetric spectrometry or optodes, e.g., Clarke et al., 2017) have matured to the extent they are now optionally included on floats, at fixed-point observatories or on VOSs. Sensors for dissolved inorganic carbon, total alkalinity, and the nutrients phosphate and silicate are also undergoing rapid development that means they will soon also become available for deployment on diverse platforms. Autonomous water samplers have also been increasingly deployed on moorings on multiple timescales to capture discrete seawater biogeochemical time series (Eriksen et al., 2018; Shamberger et al., 2011).

As yet though, deployment across TMAs observing the AMOC has been limited, with major basinwide arrays typically not including biogeochemical measurements. One exception, however, is the RAPID array, where as part of the Atlantic Biogeochemical Fluxes project, a biogeochemical element is being added: Oxygen sensors have been attached to four RAPID moorings, with pCO_2 and pH sensors and autonomous water samplers additionally located at the moorings' shallowest expression, while also, full-depth bimonthly sampling is taking place for the inorganic carbon system and inorganic and organic nutrients across Florida Straits, taking advantage of the frequent undersea cable calibration cruises. As well as the time series sites mentioned above, a number of other moorings also measure for the biogeochemical system, with the Ocean Observatories Initiative (OOI) maintaining systems in the Irminger Sea and the off the East Coast of the United States by Cape Cod; in the Labrador Sea, a SeaCycler mooring enables high vertical resolution measurements for a suite of biogeochemical sensors; in the Norwegian Sea, Station M tracks a changing carbon system and hydrographic variability; while in Fram Strait and the central Arctic, long-term biogeochemical observatories) track the interchange of waters between the Arctic and North Atlantic.

With the advent of novel, cheaper and more technologically mature biogeochemical sensors, a tremendous opportunity is opening up to investigate the relationship between ocean circulation and biogeochemistry, using both existing infrastructure and newer platforms. Our current understanding of how the two interact is based on sporadic, ship-based and temporally separated data sets, and it is of greatest importance for our understanding of how the carbon cycle and ecosystems will respond to a changing climate to better resolve the forcings, drivers and feedbacks of these climatically important processes. However, compared to the sensor-based measurement of physical characteristics and ocean currents, biogeochemical sensors are in their infancy.

7. Future Outlook and Sustainability

The goal of this paper has been to review the technologies and methodologies for observing the strength and, to a lesser extent, the associated heat, freshwater, and other fluxes of the AMOC. We will consider three questions to frame the summary in this final section:

1. How do you measure the AMOC (how-to)?
2. Why do you measure the AMOC (why)?
3. How much should an AMOC observing system cost (how-much)?

In its very simplest form, the AMOC is ocean circulation with flows in opposing meridional directions at different depths. The first minimum requirement to observe is therefore an estimation of this velocity. This

"how-to" question is also tied up with the second question "why"? The second question asks about the motivation to observe the AMOC. The primary motivation for observing the AMOC is because it plays an important role in the climate system due to its heat, freshwater, and carbon transport and is expected to change in the coming decades due to anthropogenic climate change. Therefore, the minimum requirements for observing the AMOC are an estimation of the strength of the circulation that can inform about AMOC variability on climate relevant timescales.

Using these two questions, we can summarize the methodology and technology described in this paper. The third question (how-much) is outside of the scope of the paper in a quantitative sense, but it is difficult to summarize the paper without reference to it. The reason we need to consider this question is that to observe the AMOC on climate relevant timescales, we need a system sustainable for decades and therefore optimizing the cost is crucial. Also, without cost as a consideration, the answer would be easy: We know how to measure ocean velocity accurately and continuously. An ocean filled with full depth current meter moorings, colocated with temperature, salinity, and biogeochemical measurements would provide an estimate of ocean velocity at every point in longitude, latitude, depth, and time would fully answer all of these questions. Of course, this would be prohibitively expensive and logistically wildly unfeasible.

Dedicated AMOC observing programs focus on specific zonal or quasi-zonal sections for estimating the meridional transport with TMAs. None of the basinwide systems are fully based on direct current meter observations due to the prohibitive cost and density of moorings required. Full current meter arrays are deployed in either topographically restricted areas such as the deep channels of the GSR, in strong current systems such as at 11°S, or as a (small) section of a wider array such as with RAPID and OSNAP (Figure 1 for locations).

To reduce the necessary sampling interval in longitude, the geostrophic assumption is vital. Equation (6) shows that for geostrophically balanced flow with no topographic obstacles, it is sufficient to measure dynamic height at the end points of each zonal section (section 3.2). This allows much larger spacing between moorings. Difficulties with this approach include solving for a reference velocity and dealing with non-vertical topography (section 5.2). Just as there are no basinwide arrays that observe the AMOC solely with current meters, there are no basinwide arrays that observe the AMOC solely with dynamic height moorings or geostrophy-based systems.

Further simplifications to the principle of using dynamic height can be made with PIES or SSH. Dynamic height estimates can be made using pressure inverted echo sounders (PIES, section 3.4), which utilize travel time of an acoustic pulse from the seafloor to the surface. These are widely employed in the arrays of SAMBA and NOAC. They provide an economical estimate of the dynamic height profile provided there exists a unique relationship between the acoustic travel time (equation (9)) and the dynamic height profile. Estimations of the AMOC can be made using remotely sensed estimates of SSH (section 4) along similar principles. Utilization of SSH to estimate dynamic height at the surface (including bottom pressure), bears many similarities with PIES as it used a single measurement to characterize the full water column. These estimates could be considered as having zero cost as these observations are already being made. A number of estimates of the AMOC using techniques combining SSH and Argo have been made (section 4). However, concerns exist regarding the ability of SSH and PIES to resolve shear reversal at depth and about the ability of Argo to get sufficiently close to the boundaries to make the measurements of deep flow that are necessary to estimate the AMOC. And satellite methods do not have the temporal resolution to observe the highest frequency AMOC observations observed by the moored arrays.

Geostrophy is certainly a simplifying factor for reducing the observing effort in the open ocean. However, where heat, freshwater, and other fluxes are ultimately of interest, sufficient observations of the associated properties: temperature, salinity, and, increasingly, biogeochemical properties need to be made as well.

The AMOC observing systems can be considered in the following order in relation to existing TMAs (Figure 1), in nominal order of increasing cost:

- Remotely sensed (i.e., already paid for)
- PIES and remote sensed/model, for example, SAMBA
- PIES and current meters, for example, NOAC
- Dynamic height alone, for example, MOVE

- Dynamic height and current meters (and cable/glider), for example, RAPID, OSNAP, TSAA
- All current meters/ADCP, for example, GSR overflows.

We have not considered in this review the latitudinal frequency the arrays would need to fully observe the AMOC. Looking at Figure 1, TMAs are distributed approximately every 10° to 20° of latitude, with increasing frequency in the North Atlantic. Simple concepts of the AMOC as a single conveyor belt (Broeker, 1991) are now replaced with a more nuanced understanding of differing AMOC dynamics in different ocean basins (Bingham et al., 2007; Williams et al., 2014). A consideration of how many of these observing arrays are optimal is beyond the scope here but should be considered in any Atlantic Observing Blueprint (deYoung et al., 2019; Frajka-Williams et al., 2019).

Ocean observing technology is advancing apace. Innovations in mooring technology focused on data delivery and security offer potential flexibility in deployment that could lead to significant savings and contribute to the sustainability of this traditional form of AMOC observing. Glider technology offers entirely new methods of observing the AMOC. While this technology is only now approaching the instrument stability and endurance necessary to make ocean circulation estimates, this will only improve in the future. Additional technologies, such as those from Volunteering Observing Ships, could feed into remotely sensed estimations of the AMOC or form part of a dedicated observing system. The evolution of technology has always played a role in the evolution of observing systems, for example, the change from using in situ observations only to the combination of in situ and altimetry observations in the GSR TMAs (Berx et al., 2013; Hansen et al., 2015). As technology emerges and becomes more reliable, AMOC observing systems will evolve and care will be needed to ensure a consistent transition between differing observing systems.

Biogeochemical technology (section 6.2.2) is another emerging technology, which offers exciting future possibilities for AMOC observing. In particular, the role of the AMOC in sequestering atmospheric CO_2 is a pressing issue for climate science. Compared to the physical measurements, this technology is in its infancy but offers important insights as it matures.

The aim of this paper has been to review the technology and methodologies of estimating the AMOC and to highlight emerging developments and observational gaps. Observations of the AMOC and interest in these observations have increased greatly in the last decade of the 20th and first decades of the 21st century. Motivated by the climatic importance and vulnerability to climate change of the AMOC, observing systems have been deployed throughout the Atlantic. Sustenance of this effort will hopefully mean that questions about the role of the AMOC in climate phenomena such as the warming hole in the North Atlantic (Drijfhout et al., 2012) or the Atlantic Multidecadal Variability (Clement et al., 2015) will be able to be answered definitively in the future, provided these observing systems are sustained. However, there are still gaps in the observing system such as those highlighted on the shelf and shelf edge, especially in eastern boundary regions, and the deep ocean (section 6.1). Efforts are ongoing to provide a blueprint for observing the Atlantic and the question of how to optimize and improve observations of the AMOC will be an important part of this process.

Acronyms

AABW	Antarctic Bottom Water
ADCP	Acoustic Doppler current profiler
AMOC	Atlantic Meridional Overturning Circulation
ASV	Autonomous surface vehicle
AUV	Autonomous underwater vehicle
BPR	Bottom pressure recorder
CFC	Chlorofluorocarbon
CMEMS	Copernicus Marine Environmental Monitoring Service
CMIP5	Coupled Model Intercomparison Project 5
CTD	Conductivity-temperature-depth
DAC	Depth averaged current
GEM	Gravest empirical mode
GO-SHIP	Shipboard hydrography coordination group
GOOS	Global Ocean Observing System

GPS	Global Positioning System
GRACE	The Gravity Recovery and Climate Experiment
GSR	Greenland-Scotland Ridge
IOC	International Oceanographic Commission
LADCP	Lowered acoustic Doppler current profiler
MADT	Mean absolute dynamic topography
MicroCAT	Moored CTD instrument
MOVE	The MOVE array at 16°N
NAC	North Atlantic Current
NADW	North Atlantic Deep Water
NOAC	Transport Mooring Array at 47°N
OOI	Ocean Observatories Initiative
OSNAP	Overturning in the Subpolar North Atlantic Array near 57°N
OVIDE	The OVIDE hydrographic section from Portugal to Lisbon
PAP	Porcupine abyssal plain
pCO2	Partial pressure of carbon dioxide (in seawater)
PIES	Pressure inverted echo sounders
RAPID	The RAPID/MOCHA/WBTS array at 26.5°N
SAMBA	South Atlantic Moored Buoy Array at 34.5°S
Sv	Sverdrup = 106 m3/s
TAO	Tropical Atmosphere Ocean Array
TSAA	Tropical South Atlantic Array at 11°S
UHDAS	University of Hawaii Data Acquisition System
VOS	Volunteer observing ship
WAVE	West Atlantic Variability Experiment
WMO	World Meteorological Organization
WOCE	World Ocean Circulation Experiment

Acknowledgments
This work was supported by EU Horizon 2020 project AtlantOS (Grant 633211) and Blue-Action (Grant 727852), and EU FP7 project NACLIM. G. M. was supported by the A4 project (Grant Aid Agreement PBA/CC/18/01) supported by the Irish Marine Institute under the Marine Research Programme funded by the Irish Government, cofinanced by the ERDF. R. H. was supported by German Federal Ministry of Education and Research as part of the cooperative project RACE (03F0605B). G. G., C. S., and C. S. M. acknowledge support from NOAA (CPO-OOMD and AOML). The 47°N array NOAC is funded by the German Ministry of Education and Research (BMBF) with Grants 03F0443C, 03F0605C, 03F0561C, and 03F0792A to M. R. The Senate Commission of Oceanography from the National Science Foundation (DFG) granted ship time and costs for travel, transports, and consumables to M. R. P. J. B. was supported by the U.K. Natural Environment Research Council through projects "Radiatively Active Gases from the North Atlantic Region and Climate Change" (RAGNARoCC) NE/K00249X/1 and "Atlantic Biogeochemical Fluxes" (ABC-Fluxes) NE/M005046/1. No new data were used in this study.

References

Almeida, L., de Azevedo, J. L. L., Kerr, R., Araujo, M., & Mata, M. M. (2018). Impact of the new equation of state of seawater (TEOS-10) on the estimates of water mass mixture and meridional transport in the Atlantic Ocean. *Progress in Oceanography*. https://doi.org/10.1016/j.pocean.2018.02.008

Andres, M. (2016). On the recent destabilization of the Gulf Stream path downstream of Cape Hatteras. *Geophysical Research Letters*, *43*, 9836–9842. https://doi.org/10.1002/2016gl069966

Baehr, J., Hirschi, J., Beismann, J.-O., & Marotzke, J. (2004). Monitoring the meridional overturning circulation in the North Atlantic: A model-based array design study. *Journal of Marine Research*, *62*, 283–312. https://doi.org/10.1357/0022240041446191

Barnes, C. R., 2007: Building the world's first regional cabled ocean observatory (NEPTUNE): Realities, challenges and opportunities. Oceans Conference Record (IEEE).

Beal, L. M., Elipot, S., Houk, A., & Leber, G. M. (2015). Capturing the transport variability of a western boundary jet: Results from the Agulhas Current Time-Series Experiment (ACT)*. *Journal of Physical Oceanography*, *45*, 1302–1324. https://doi.org/10.1175/JPO-D-14-0119.1

Berx, B., Hansen, B., Østerhus, S., Larsen, K. M., Sherwin, T., & Jochumsen, K. (2013). Combining in-situ measurements and altimetry to estimate volume, heat and salt transport variability through the Faroe Shetland Channel. *Ocean Science*, *9*, 639–654. https://doi.org/10.5194/os-9-639-2013

Biastoch, A., Boning, C. W., & Lutjeharms, J. R. E. (2008). {A}gulhas leakage dynamics affects decadal variability in {A}tlantic overturning circualtion. *Nature*, *456*(7221), 489–492. https://doi.org/10.1038/nature07426

Bingham, C. W., & Hughes, J. (2009). Geostrophic dynamics of meridional transport variability in the subpolar North Atlantic. *Journal of Geophysical Research, Oceans*, *114*, 1–17. https://doi.org/10.1029/2009JC005492

Bingham, R. J., & Hughes, C. W. (2008). Determining North Atlantic meridional transport variability from pressure on the western boundary: A model investigation. *Journal of Geophysical Research, Oceans*, *113*. https://doi.org/10.1029/2007JC004679

Bingham, R. J., Hughes, C. W., Roussenov, V., & Williams, R. G. (2007). Meridional coherence of the North Atlantic meridional overturning circulation. *Geophysical Research Letters*, *34*, L23606. https://doi.org/10.1029/2007gl031731

Bower, A. S., Lozier, M. S., Gary, S. F., & Böning, C. W. (2009). Interior pathways of the North Atlantic meridional overturning circulation. *Nature*. https://doi.org/10.1038/nature07979

Brandt, P., Funk, A., Tantet, A., Johns, W. E., & Fischer, J. (2014). The Equatorial Undercurrent in the central Atlantic and its relation to tropical Atlantic variability. *Climate Dynamics*, *43*(11), 2985–2997. https://doi.org/10.1007/s00382-014-2061-4

Bresnahan, P. J., Martz, T. R., Takeshita, Y., Johnson, K. S., & LaShomb, M. (2014). Best practices for autonomous measurement of sea-water pH with the Honeywell Durafet. *Methods in Oceanography*. https://doi.org/10.1016/j.mio.2014.08.003

Brink, K. H., & Kirincich, A. R. (2017). Some considerations about coastal ocean observing systems. *Journal of Marine Research*. https://doi.org/10.1357/002224017821836743

Brito, M., Smeed, D., & Griffiths, G. (2014). Underwater glider reliability and implications for survey design. *Journal of Atmospheric and Oceanic Technology*. https://doi.org/10.1175/JTECH-D-13-00138.1

Broecker, W. S., & Peng, T. H. (1992). Interhemispheric transport of carbon dioxide by ocean circulation. *Nature*. https://doi.org/10.1038/356587a0

Broeker, W. S. (1991). The Great Ocean Conveyor. *Oceanography*, *4*, 79–89. https://doi.org/10.5670/oceanog.1991.07

Bryden, H. L., & Hall, M. M. (1980). Heat transport by currents across 25°N latitude in the Atlantic Ocean. *Science (80-.)*, *207*, 884–886. https://doi.org/10.1126/science.207.4433.884

Bryden, H. L., & Imawaki, S. (2001). Ocean heat transport. *International Geophysics Series*, *77*, 454–477

Bryden, H. L., Longworth, H. R., & Cunningham, S. A. (2005). Slowing of the Atlantic meridional overturning circulation at 25°N. *Nature*, *438*(7068), 655–657. https://doi.org/10.1038/nature04385

Bryden, H. L., Mujahid, A., Cunningham, S. A., & Kanzow, T. (2009). Adjustment of the basin-scale circulation at 26°N to variations in Gulf Stream, Deep Western Boundary Current and Ekman transports as observed by the RAPID array. *Journal of Geophysical Research Ocean Science*, *5*, 421–433. https://doi.org/10.5194/os-5-421-2009

Bushinsky, S. M., Gray, A. R., Johnson, K. S., & Sarmiento, J. L. (2017). Oxygen in the Southern Ocean from Argo Floats: Determination of processes driving air-sea fluxes. *Journal of Geophysical Research: Oceans*, *122*, 8661–8682. https://doi.org/10.1002/2017JC012923

Clarke, J. S., Achterberg, E. P., Connelly, D. P., Schuster, U., & Mowlem, M. (2017). Developments in marine pCO_2 measurement technology; towards sustained in situ observations. *TrAC, Trends in Analytical Chemistry*. https://doi.org/10.1016/j.trac.2016.12.008

Clement, A., Bellomo, K., Murphy, L. N., Cane, M. A., Mauritsen, T., Rädel, G., & Stevens, B. (2015). The Atlantic Multidecadal Oscillation without a role for ocean circulation. *Science (80-.)*, *350*, 320–324. https://doi.org/10.1126/science.aab3980

Cullison Gray, S. E., DeGrandpre, M. D., Moore, T. S., Martz, T. R., Friederich, G. E., & Johnson, K. S. (2011). Applications of in situ pH measurements for inorganic carbon calculations. *Marine Chemistry*. https://doi.org/10.1016/j.marchem.2011.02.005

Cunningham, S. A., Kanzow, T., Rayner, D., Baringer, M. O., Johns, W. E., Marotzke, J., et al. (2007). Temporal variability of the Atlantic Meridional Overturning Circulation at 26.5°N. *Science (80-.)*, *317*, 935–938. https://doi.org/10.1126/science.1141304

Curry, B., Lee, C. M., Petrie, B., Moritz, R. E., & Kwok, R. (2014). Multiyear volume, liquid freshwater, and sea ice transports through Davis Strait, 2004–10*. *Journal of Physical Oceanography*. https://doi.org/10.1175/JPO-D-13-0177.1

Dansgaard, W., Johnsen, S. J., Clausen, H. B., Dahl-Jensen, D., Gundestrup, N. S., Hammer, C. U., et al. (1993). Evidence for general instability of past climate from a 250-kyr ice-core record. *Nature*, *364*, 218–220. https://doi.org/10.1038/364218a0

de Jong, M. F., Oltmanns, M., Karstensen, J., & de Steur, L. (2018). Deep Convection in the Irminger Sea Observed with a Dense Mooring Array. *Oceanography*. https://doi.org/10.5670/oceanog.2018.109

Dee, D. P., Uppala, S. M., Simmons, A. J., Berrisford, P., Poli, P., Kobayashi, S., et al. (2011). The ERA-Interim reanalysis: Configuration and performance of the data assimilation system. *Quarterly Journal of the Royal Meteorological Society*, *137*, 553–597. https://doi.org/10.1002/qj.828

Dengler, M., Schott, F. A., Eden, C., Brandt, P., Fischer, J., & Zantopp, R. J. (2004). Break-up of the Atlantic Deep Western Boundary Current into eddies at 8° S. *Nature*, *432*(7020), 1018–1020. https://doi.org/10.1038/nature03134

DeVries, T., Holzer, M., & Primeau, F. (2017). Recent increase in oceanic carbon uptake driven by weaker upper-ocean overturning. *Nature*, *542*(7640), 215–218. https://doi.org/10.1038/nature21068

deYoung, B., Visbeck, M., de Araujo Filho, M. C., Baringer, M. O., Black, C., Buch, E., et al. (2019). An integrated all-Atlantic ocean observing system in 2030. *Frontiers in Marine Science*. https://doi.org/10.3389/fmars.2019.00428

Dong, S.,Goni, G., & Bringas, F. (2015). Temporal variability of the Meridional Overturning Circulation in the South Atlantic between 20S and 35S. *Geophysical Research Letters*, *42*, 7655–7662. https://doi.org/10.1002/2015GL065603

Donners, J., & Drijfhout, S. S. (2004). The Lagrangian view of South Atlantic interocean exchange in a global ocean model compared with inverse model results. *Journal of Physical Oceanography*, *34*, 1019–1035. https://doi.org/10.1175/1520-0485(2004)034<1019:tlvosa>2.0.co;2

Donohue, K. A., Watts, D. R., Tracey, K. L., Greene, A. D., & Kennelly, M. (2010). Mapping circulation in the Kuroshio Extension with an array of current and pressure recording inverted echo sounders. *Journal of Atmospheric and Oceanic Technology*. https://doi.org/10.1175/2009JTECHO686.1

Drijfhout, S., Oldenborgh, G. J. V., & Cimatoribus, A. (2012). Is a decline of AMOC causing the warming hole above the North Atlantic in observed and modeled warming patterns? *Journal of Climate*, *25*, 8373–8379. https://doi.org/10.1175/jcli-d-12-00490.1

Eriksen, C. C., Osse, T. J., Light, R. D., Wen, T., Lehman, T. W., Sabin, P. L., et al. (2001). Seaglider: A long-range autonomous underwater vehicle for oceanographic research. *IEEE Journal of Oceanic Engineering*. https://doi.org/10.1109/48.972073

Eriksen, R., Trull, T. W., Davies, D., Jansen, P., Davidson, A. T., Westwood, K., & Van Den Enden, R. (2018). Seasonal succession of phytoplankton community structure from autonomous sampling at the Australian Southern Ocean Time Series (SOTS) observatory. *Marine Ecology Progress Series*. https://doi.org/10.3354/meps12420

Firing, E. (1991). Acoustic Doppler profiling measurements and navigation. WHP Hydrographic Operations and Methods. http://geo.h2o.ucsd.edu/documentation/manuals/pdf/91_1/firadcp.pdf

Fischer, J., & Schott, F. A. (2002). Labrador Sea water tracked by profiling floats—From the boundary current into the open North Atlantic. *Journal of Physical Oceanography*. https://doi.org/10.1175/1520-0485(2002)032<0573:LSWTBP>2.0.CO;2

Fischer, J., Schott, F. A., & Dengler, M. (2004). Boundary circulation at the exit of the Labrador Sea. *Journal of Physical Oceanography*. https://doi.org/10.1109/RAMS.2015.7105091

Flagg, C. N., Schwartze, G., Gottlieb, E., & Rossby, T. (1998). Operating an acoustic Doppler current profiler aboard a container vessel. *Journal of Atmospheric and Oceanic Technology*, *15*, 257–271. https://doi.org/10.1175/1520-0426(1998)015<0257:oaadcp>2.0.co;2

Frajka-Williams, E. (2015). Estimating the Atlantic overturning at 26°N using satellite altimetry and cable measurements. *Geophysical Research Letters*, *42*, 3458–3464. https://doi.org/10.1002/2015GL063220

Frajka-Williams, E., Ansorge, I. J., Baehr, J., Bryden, H. L., Chidichimo, M. P., Cunningham, S. A., et al. (2019). Atlantic meridional overturning circulation: Observed transport and variability. *Frontiers in Marine Science*. https://doi.org/10.3389/fmars.2019.00260

Frajka-Williams, E., Cunningham, S. A., Bryden, H., & King, B. A. (2011). Variability of Antarctic Bottom Water at 24.5°N in the Atlantic. *Journal of Geophysical Research*, *116*, C11026. https://doi.org/10.1029/2011jc007168

Fu, Y., Karstensen, J., Brandt, P., & Kiel, C. (2017). Atlantic meridional overturning circulation at 14.5°N and 24.5°N during 1989/1992 and 2013/2015: volume, heat and freshwater fluxes. *Ocean Science Discussions*, 1–48. https://doi.org/10.5194/os-2017-87

Ganachaud, A., & Wunsch, C. (2003). Large-scale ocean heat and freshwater transports during the world ocean circulation experiment. *Journal of Climate*. https://doi.org/10.1175/1520-0442(2003)016<0696:LSOHAF>2.0.CO;2

Garcia, R. F., & Meinen, C. S. (2014). Accuracy of Florida Current volume transport measurements at 27°N using multiple observational techniques. *Journal of Atmospheric and Oceanic Technology*, *31*(5), 1169–1180. https://doi.org/10.1175/JTECH-D-13-00148.1

Garzoli, S. L., & Baringer, M. O. (2007). Meridional heat transport determined with expandable bathythermographs—Part II: South Atlantic transport. *Deep Sea Research Part I: Oceanographic Research Papers*. https://doi.org/10.1016/j.dsr.2007.04.013

Goni, G., Kamholz, S., Garzoli, S., & Olson, D. (1996). Dynamics of the Brazil-Malvinas confluence based on inverted echo sounders and altimetry. *Journal of Geophysical Research Oceans*. https://doi.org/10.1029/96JC01146

Gordon, A. L. (1986). Interocean exchange of thermocline water. *Journal of Geophysical Research*, *91*, 5037–5046. https://doi.org/10.1029/jc091ic04p05037

Haine, T. W. N., Curry, B., Gerdes, R., Hansen, E., Karcher, M., Lee, C., et al. (2015). Arctic freshwater export: Status, mechanisms, and prospects. *Global and Planetary Change*, *125*, 13–35. https://doi.org/10.1016/j.gloplacha.2014.11.013

Haines, K., Stepanov, V. N., Valdivieso, M., & Zuo, H. (2013). Atlantic meridional heat transports in two ocean reanalyses evaluated against the RAPID array. *Geophysical Research Letters*, *40*, 343–348. https://doi.org/10.1029/2012gl054581

Hall, M. M., & Bryden, H. L. (1982). Direct estimates and mechanisms of ocean heat transport. *Deep Sea Research Part A. Oceanographic Research Papers*, *29*, 339–359. https://doi.org/10.1016/0198-0149(82)90099-1

Hansen, B., Hátún, H., Kristiansen, R., Olsen, S. M., & Osterhus, S. (2010). Stability and forcing of the Iceland-Faroe inflow of water, heat, and salt to the Arctic. *Ocean Science*, *6*, 1013–1026. https://doi.org/10.5194/os-6-1013-2010

Hansen, B., Larsen, K. M. H., Hátún, H., Kristiansen, R., Mortensen, E., & Østerhus, S. (2015). Transport of volume, heat, and salt towards the Arctic in the Faroe Current 1993-2013. *Ocean Science*. https://doi.org/10.5194/os-11-743-2015

Hansen, B., Larsen, K. M. H., Hátún, H., & Østerhus, S. (2016). A stable Faroe Bank Channel overflow 1995-2015. *Ocean Science*. https://doi.org/10.5194/os-12-1205-2016

Hansen, B., & Østerhus, S. (2000). North Atlantic-Nordic Seas exchanges. *Progress in Oceanography*, *45*, 109–208. https://doi.org/10.1016/s0079-6611(99)00052-x

Hernández-Guerra, A., Pelegrí, J. L., Fraile-Nuez, E., Benítez-Barrios, V., Emelianov, M., Pérez-Hernández, M. D., & Vélez-Belchí, P. (2014). Meridional overturning transports at 7.5°N and 24.5°N in the Atlantic Ocean during 1992–93 and 2010–11. *Progress in Oceanography*, *128*, 98–114. https://doi.org/10.1016/j.pocean.2014.08.016

Hirschi, J., Baehr, J., Marotzke, J., Stark, J., Cunningham, S., & Beismann, J.-O. (2003). A monitoring design for the Atlantic meridional overturning circulation. *Geophysical Research Letters*, *30*(7), 1413 https://doi.org/10.1029/2002gl016776

Hogg, N. G., & Frye, D. E. (2007). Performance of a new generation of acoustic current meters. *Journal of Physical Oceanography*. https://doi.org/10.1175/JPO3003.1

Holfort, J., Johnson, K. M., Schneider, B., Siedler, G., & Wallace, D. W. R. (1998). Meridional transport of dissolved inorganic carbon in the South Atlantic Ocean. *Global Biogeochemical Cycles*. https://doi.org/10.1029/98GB01533

Holliday, N. P., Bacon, S., Cunningham, S. A., Gary, S. F., Karstensen, J., King, B. A., et al. (2018). Subpolar North Atlantic Overturning and gyre-scale circulation in the summers of 2014 and 2016. *Journal of Geophysical Research: Oceans*, *123*, 4538–4559. https://doi.org/10.1029/2018JC013841

Holt, J., Polton, J., Huthnance, J., Wakelin, S., O'Dea, E., Harle, J., et al. (2018). Climate-driven change in the North Atlantic and Arctic Ocean can greatly reduce the circulation of the North Sea. *Geophysical Research Letters*, *1–10*. https://doi.org/10.1029/2018GL078878

Houpert, L., Inall, M. E., Dumont, E., Gary, S., Johnson, C., Porter, M., et al. (2018). Structure and transport of the North Atlantic Current in the eastern subpolar gyre from sustained glider observations. *Journal of Geophysical Research: Oceans*. https://doi.org/10.1029/2018JC014162

Howe, B. M., Arbic, B. K., Aucan, J., Barnes, C. R., Bayliff, N., Becker, N., et al. (2019). SMART Cables for observing the global ocean: Science and implementation. *Frontiers in Marine Science*. https://doi.org/10.3389/fmars.2019.00424

Hughes, C. W., Elipot, S., Morales Maqueda, M. Á., & Loder, J. W. (2013). Test of a method for monitoring the geostrophic meridional overturning circulation using only boundary measurements. *Journal of Atmospheric and Oceanic Technology*, *30*, 789–809. https://doi.org/10.1175/jtech-d-12-00149.1

Hughes, C. W., Williams, J., Blaker, A., Coward, A., & Stepanov, V. (2018). A window on the deep ocean: The special value of ocean bottom pressure for monitoring the large-scale, deep-ocean circulation. *Progress in Oceanography*. https://doi.org/10.1016/j.pocean.2018.01.011

Hummels, R., Brandt, P., Dengler, M., Fischer, J., Araujo, M., Veleda, D., & Durgadoo, J. V. (2015). Interannual to decadal changes in the western boundary circulation in the Atlantic at 11°S. *Geophysical Research Letters*, *42*, 7615–7622. https://doi.org/10.1002/2015GL065254

IOC, SCOR, and IAPSO (2010). *The international thermodynamic equation of seawater 2010: Calculation and use of thermodynamic properties, Intergovernmental Oceanographic Commission, Manuals and Guides No. 56*. UNESCO. (English)

Jackson, L. C., Kahana, R., Graham, T., Ringer, M. A., Woollings, T., Mecking, J. V., & Wood, R. A. (2015). Global and European climate impacts of a slowdown of the AMOC in a high resolution GCM. *Climate Dynamics*. https://doi.org/10.1007/s00382-015-2540-2

Jochumsen, K., Moritz, M., Nunes, N., Quadfasel, D., Larsen, K. M. H., Hansen, B., et al. (2017). Revised transport estimates of the Denmark Strait overflow. *Journal of Geophysical Research: Oceans*, *122*, 3434–3450. https://doi.org/10.1002/2017JC012803

Jochumsen, K., Quadfasel, D., Valdimarsson, H., & Jonsson, S. (2012). Variability of the Denmark Strait overflow: Moored time series from 1996–2011. *Journal of Geophysical Research, Oceans*, *117*. https://doi.org/10.1029/2012jc008244

Johns, W. E., Beal, L. M., Baringer, M. O., Molina, J. R., Cunningham, S. A., Kanzow, T., & Rayner, D. (2008). Variability of shallow and Deep Western Boundary Currents off the Bahamas during 2004-05: Results from the 26°N RAPID-MOC array. *Journal of Physical Oceanography*, *38*, 605–623. https://doi.org/10.1175/2007JPO3791.1

Johns, W. E., Kanzow, T., & Zantopp, R. (2005). Estimating ocean transports with dynamic height moorings: An application in the Atlantic Deep Western Boundary Current at 26°N. *Deep Sea Research Part I: Oceanographic Research Papers*, *52*, 1542–1567. https://doi.org/10.1016/j.dsr.2005.02.002

Johnson, G. C., Rudnick, D. L., & Taft, B. A. (1994). Bottom water variability in the Samoa Passage. *Journal of Marine Research*. https://doi.org/10.1357/0022240943077118

Johnson, K. S., Plant, J. N., Dunne, J. P., Talley, L. D., & Sarmiento, J. L. (2017). Annual nitrate drawdown observed by SOCCOM profiling floats and the relationship to annual net community production. *Journal of Geophysical Research: Oceans*, *122*, 6668–6683. https://doi.org/10.1002/2017JC012839

Kajikawa, H., & Kobata, T. (2014). Reproducibility of calibration results by 0-A-0 pressurization procedures for hydraulic pressure transducers. *Measurement Science and Technology*. https://doi.org/10.1088/0957-0233/25/1/015008

Kanzow, T., Cunningham, S. A., Johns, W. E., Hirschi, J. J.-M., Marotzke, J., Baringer, M. O., et al. (2010). Seasonal variability of the Atlantic Meridional Overturning Circulation at 26.5°N. *Journal of Climate*, *23*, 5678–5698. https://doi.org/10.1175/2010JCLI3389.1

Kanzow, T., Cunningham, S. A., Rayner, D., Hirschi, J. J.-M., Johns, W. E., Baringer, M. O., et al. (2007). Observed flow compensation associated with the MOC at 26.5°N in the Atlantic. *Science (80-.)*, *317*, 938–941. https://doi.org/10.1126/science.1141293 http://www.sciencemag.org/content/317/5840/938.abstract

Kanzow, T., Johnson, H. L., Marshall, D. P., Cunningham, S. A., Hirschi, J.-M., Mujahid, A., et al. (2009). Basinwide integrated volume transports in an eddy-filled ocean. *Journal of Physical Oceanography*, *39*, 3091–3110. https://doi.org/10.1175/2009jpo4185.1

Kelley, D. S., Delaney, J. R., & Juniper, S. K. (2014). Establishing a new era of submarine volcanic observatories: Cabling Axial Seamount and the Endeavour Segment of the Juan de Fuca Ridge. *Marine Geology*. https://doi.org/10.1016/j.margeo.2014.03.010

Körtzinger, A., Schimanski, J., Send, U., & Wallace, D. (2004). The ocean takes a deep breath. *Science (80-.)*. https://doi.org/10.1126/science.1102557

Landerer, F. W., Wiese, D. N., Bentel, K., Boening, C., & Watkins, M. M. (2015). North Atlantic meridional overturning circulation variations from GRACE ocean bottom pressure anomalies. *Geophysical Research Letters*, *42*, 8114–8121. https://doi.org/10.1002/2015GL065730

Larsen, J. (1992). Transport and heat flux of the Florida current at 27°N derived from cross-stream voltages and profiling data: Theory and observations. *Deep Sea Research Part I: Oceanographic Research Papers*, *338*(1650), 169–236. https://doi.org/10.1098/rsta.1992.0007

Larsen, J. C., & Sanford, T. B. (1985). Florida current volume transports from voltage measurements. *Science (80-.)*. https://doi.org/10.1126/science.227.4684.302

Laxenaire, R., Speich, S., Blanke, B., Chaigneau, A., Pegliasco, C., & Stegner, A. (2018). Anticyclonic eddies connecting the western boundaries of Indian and Atlantic Oceans. *Journal of Geophysical Research: Oceans*. https://doi.org/10.1029/2018JC014270

Liblik, T., Karstensen, J., Testor, P., Alenius, P., Hayes, D., Ruiz, S., et al. (2016). Potential for an underwater glider component as part of the Global Ocean Observing System. *Methods in Oceanography*, *17*, 50–82. https://doi.org/10.1016/j.mio.2016.05.001

Locarnini, R. A., Mishonov, A. V., Antonov, J. I., Boyer, T. P., Garcia, H. E., Baranova, O. K., et al. (2013). World Ocean Atlas 2013. In S. Levitus (Ed.), A. Mishonov, Technical Ed.*Temperature*, (Vol. *1*). NOAA Atlas NESDIS.

Lopez, H., Dong, S., Lee, S. K., & Goni, G. (2016). Decadal modulations of interhemispheric global atmospheric circulations and monsoons by the South Atlantic meridional overturning circulation. *Journal of Climate*. https://doi.org/10.1175/JCLI-D-15-0491.1

Lozier, M. S., Bacon, S., Bower, A. S., Cunningham, S. A., Femke de Jong, M., de Steur, L., et al. (2017). Overturning in the subpolar North Atlantic program: A new international ocean observing system. *Bulletin of the American Meteorological Society*. https://doi.org/10.1175/BAMS-D-16-0057.1

Lozier, M. S., Li, F., Bacon, S., Bahr, F., Bower, A. S., Cunningham, S. A., et al. (2019). A sea change in our view of overturning in the subpolar North Atlantic. *Science (80-.)*, *363*(6426), 516–521. https://doi.org/10.1126/science.aau6592

Macdonald, A. M., Baringer, M. O., Wanninkhof, R., Lee, K., & Wallace, D. W. R. (2003). A 1998-1992 comparison of inorganic carbon and its transport across 24.5°N in the Atlantic. *Deep Sea Research Part II: Topical Studies in Oceanography*. https://doi.org/10.1016/j.dsr2.2003.07.009

Macdonald, A. M., & Wunsch, C. (1996). An estimate of global ocean circulation and heat fluxes. *Nature*. https://doi.org/10.1038/382436a0

Majumder, S., Schmid, C., & Halliwell, G. (2016). An observations and model-based analysis of meridional transports in the South Atlantic. *Journal of Geophysical Research: Oceans*, *121*, 5622–5638. https://doi.org/10.1002/2016JC011693

Martz, T. R., Connery, J. G., & Johnson, K. S. (2010). Testing the Honeywell Durafet® for seawater pH applications. *Limnology and Oceanography: Methods*. https://doi.org/10.4319/lom.2010.8.172

Maury, M. F. (1855). *The physical geography of the sea and its meteorology*. New York: Harper Brother.

McCarthy, G. D., Gleeson, E., & Walsh, S. (2015). The influence of ocean variations on the climate of Ireland. *Weather*, *70*, 242–245. https://doi.org/10.1002/wea.2543

McCarthy, G. D., Menary, M. B., Mecking, J. V., Moat, B. I., Johns, W. E., Andrews, M. B., et al. (2017). The importance of deep, basinwide measurements in optimized Atlantic Meridional Overturning Circulation observing arrays. *Journal of Geophysical Research: Oceans*, *122*, 1808–1826. https://doi.org/10.1002/2016JC012200

McCarthy, G. D., Smeed, D. A., Johns, W. E., Frajka-Williams, E., Moat, B. I., Rayner, D., et al. (2015). Measuring the Atlantic Meridional Overturning Circulation at 26°N. *Progress in Oceanography*, *31*, 91–111. https://doi.org/10.1016/j.pocean.2014.10.006

McPhaden, M. J., Ando, K., Bourles, B., Freitag, H. P., Lumpkin, R., Masumoto, Y., et al. (2010). The global tropical moored buoy array. *Proceedings of OceanObs's09: Sustained Ocean Observations and Information for Society*, *9*. https://doi.org/10.5270/OceanObs09.cwp.61

Meinen, C. S., Baringer, M. O., & Garcia, R. F. (2010). Florida Current transport variability: An analysis of annual and longer-period signals. *Deep Sea Research Part I: Oceanographic Research Papers*, *57*, 835–846. https://doi.org/10.1016/j.dsr.2010.04.001

Meinen, C. S., Johns, W. E., Garzoli, S. L., van Sebille, E., Rayner, D., Kanzow, T., & Baringer, M. O. (2013). Variability of the Deep Western Boundary Current at 26.5°N during 2004–2009. *Deep Sea Research Part II: Topical Studies in Oceanography*, *85*, 154–168. https://doi.org/10.1016/j.dsr2.2012.07.036

Meinen, C. S., Speich, S., Perez, R. C., Dong, S., Piola, A. R., Garzoli, S. L., et al. (2013). Temporal variability of the meridional overturning circulation at 34.5°S: Results from two pilot boundary arrays in the South Atlantic. *Journal of Geophysical Research: Oceans*, *118*, 6461–6478. https://doi.org/10.1002/2013jc009228

Meinen, C. S., Speich, S., Piola, A. R., Ansorge, I., Campos, E., Kersalé, M., et al. (2018). Meridional overturning circulation transport variability at 34.5°S during 2009–2017: Baroclinic and barotropic flows and the dueling influence of the boundaries. *Geophysical Research Letters*, *45*(9), 4180–4188. https://doi.org/10.1029/2018GL077408

Meinen, C. S., & Watts, D. R. (1998). Calibrating inverted echo sounders equipped with pressure sensors. *Journal of Atmospheric and Oceanic Technology*. https://doi.org/10.1175/1520-0426(1998)015<1339:CIESEW>2.0.CO;2

Meinen, D. R., & Watts, S. (2000). Vertical structure and transport on a transect across the North Atlantic Current near 42°N: Time series and mean. *Journal of Geophysical Research Oceans*. https://doi.org/10.1029/2000JC900097

Meinen, D. R., Watts, S., Luther, D. S., & Baringer, M. O. (2009). Structure, transport and potential vorticity of the Gulf Stream at 68°W: Revisiting older data sets with new techniques. *Deep Sea Research Part I: Oceanographic Research Papers*. https://doi.org/10.1016/j.dsr.2008.07.010

Meinen, D. R., Watts, S., Randolph Watts, D., & Allyn Clarke, R. (2000). Absolutely referenced geostrophic velocity and transport on a section across the North Atlantic Current. *Deep Sea Research Part I: Oceanographic Research Papers*. https://doi.org/10.1016/S0967-0637(99)00061-8

Mensah, V., Andres, M., Lien, R. C., Ma, B., Lee, C. M., & S. (Jan, 2016). Combining observations from multiple platforms across the Kuroshio northeast of Luzon: A highlight on PIES data. *Journal of Atmospheric and Oceanic Technology*. https://doi.org/10.1175/JTECH-D-16-0095.1

Mercier, H., Lherminier, P., Sarafanov, A., Gaillard, F., Daniault, N., Desbruyères, D., et al. (2015). Variability of the meridional overturning circulation at the Greenland-Portugal OVIDE section from 1993 to 2010. *Progress in Oceanography*, *132*, 250–261. https://doi.org/10.1016/j.pocean.2013.11.001

Mertens, C., Rhein, M., Walter, M., Böning, C. W., Behrens, E., Kieke, D., et al. (2014). Circulation and transports in the Newfoundland Basin, western subpolar North Atlantic. *Journal of Geophysical Research: Oceans*, *119*, 7772–7793. https://doi.org/10.1002/2014JC010019
Mertens, C., Rhein, M., Walter, M., & Kirchner, K. (2009). Modulation of the inflow into the Caribbean Sea by North Brazil Current rings. *Deep Sea Research Part I: Oceanographic Research Papers*. https://doi.org/10.1016/j.dsr.2009.03.002
Morozov, E. G., Tarakanov, R. Y., Frey, D. I., Demidova, T. A., & Makarenko, N. I. (2018). Bottom water flows in the tropical fractures of the Northern Mid-Atlantic Ridge. *Journal of Oceanography*, *74*(2), 147–167. https://doi.org/10.1007/s10872-017-0445-x
Nilson, J. A. U., Sigray, P., & Tyler, R. H. (2007). Geoelectric monitoring of wind-driven barotropic transports in the Baltic Sea. *Journal of Atmospheric and Oceanic Technology*. https://doi.org/10.1175/JTECH2068.1
Østerhus, S., Turrell, W. R., Jónsson, S., & Hansen, B. (2005). Measured volume, heat, and salt fluxes from the Atlantic to the Arctic Mediterranean. *Geophysical Research Letters*, *32*, L07603. https://doi.org/10.1029/2004gl022188
Østerhus, S., Woodgate, R., Valdimarsson, H., Turrell, B., de Steur, L., Quadfasel, D., et al. (2019). Arctic Mediterranean exchanges: A consistent volume budget and trends in transports from two decades of observations. *Ocean Science*. https://doi.org/10.5194/os-15-379-2019
Pérez, F. F., Mercier, H., Vázquez-Rodríguez, M., Lherminier, P., Velo, A., Pardo, P. C., et al. (2013). Atlantic Ocean CO_2 uptake reduced by weakening of the meridional overturning circulation. *Nature Geoscience*. https://doi.org/10.1038/ngeo1680
Piecuch, C. G., Dangendorf, S., Ponte, R. M., & Marcos, M. (2016). Annual sea level changes on the North American Northeast Coast: Influence of local winds and barotropic motions. *Journal of Climate*, *29*, 4801–4816. https://doi.org/10.1175/jcli-d-16-0048.1
Porter, M., Dale, A. C., Jones, S., Siemering, B., & Inall, M. E. (2018). Cross-slope flow in the Atlantic Inflow Current driven by the on shelf deflection of a slope current. *Deep Sea Research Part I: Oceanographic Research Papers*, *140*, 173–185. https://doi.org/10.1016/j.dsr.2018.09.002
Rayner, D., Hirschi, J. J.-M., Kanzow, T., Johns, W. E., Wright, P. G., Frajka-Williams, E., et al. (2011). Monitoring the Atlantic meridional overturning circulationlantic meridional overturning circulation. *Deep Sea Research Part II: Topical Studies in Oceanography*, *58*, 1744–1753. https://doi.org/10.1016/j.dsr2.2010.10.056
Rennermalm, A. K., Wood, E. F., Weaver, A. J., Eby, M., & Déry, S. J. (2007). Relative sensitivity of the Atlantic meridional overturning circulation to river discharge into Hudson Bay and the Arctic Ocean. *Journal of Geophysical Research – Biogeosciences*, *112*, 1–12. https://doi.org/10.1029/2006JG000330
Rhein, M., Kieke, D., Hüttl-Kabus, S., Roessler, A., Mertens, C., Meissner, R., et al. (2011). Deep water formation, the subpolar gyre, and the meridional overturning circulation in the subpolar North Atlantic. *Deep Sea Research Part II: Topical Studies in Oceanography*. https://doi.org/10.1016/j.dsr2.2010.10.061
Rhein, M., Kieke, D., & Steinfeldt, R. (2015). Advection of North Atlantic Deep Water from the labrador sea to the southern hemisphere. *Journal of Geophysical Research, C: Oceans*. https://doi.org/10.1002/2014JC010605
Rhein, M., Mertens, C., & Roessler, A. (2019). Observed transport decline at 47°N, western Atlantic. *Journal of Geophysical Research: Oceans*, *124*. https://doi.org/10.1029/2019JC014993
Rhein, M., Steinfeldt, R., Kieke, D., Stendardo, I., & Yashayaev, I. (2017). Ventilation variability of Labrador Sea Water and its impact on oxygen and anthropogenic carbon: A review. *Philosophical Transactions of the Royal Society A - Mathematical Physical and Engineering Sciences*. https://doi.org/10.1098/rsta.2016.0321
Richardson, W. S., Stimson, P. B., & Wilkins, C. H. (1963). Current measurements from moored buoys. *Deep Sea Research and Oceanographic Abstracts*. https://doi.org/10.1016/0011-7471(63)90503-5
Rintoul, S. R. (1991). South Atlantic Interbasin Exchange. *Journal of Geophysical Research*, *96*, 2675–2692. https://doi.org/10.1029/90jc02422
Riser, S. C., Freeland, H. J., Roemmich, D., Wijffels, S., Troisi, A., Belbéoch, M., et al. (2016). Fifteen years of ocean observations with the global Argo array. *Nature Climate Change*. https://doi.org/10.1038/nclimate2872
Roessler, A., Rhein, M., Kieke, D., & Mertens, C. (2015). Long-term observations of North Atlantic Current transport at the gateway between western and eastern Atlantic. *Journal of Geophysical Research, C: Oceans*. https://doi.org/10.1002/2014JC010662
Rossby, T., & Flagg, C. N. (2012). Direct measurement of volume flux in the Faroe-Shetland Channel and over the Iceland-Faroe Ridge. *Geophysical Research Letters*, *39*, L07602. https://doi.org/10.1029/2012GL051269
Rossby, T., Flagg, C. N., Donohue, K., Sanchez-Franks, A., & Lillibridge, J. (2014). On the long-term stability of Gulf Stream transport based on 20 years of direct measurements. *Geophysical Research Letters*, *41*, 114–120. https://doi.org/10.1002/2013GL058636
Roussenov, V. M., Williams, R. G., Hughes, C. W., & Bingham, R. J. (2008). Boundary wave communication of bottom pressure and overturning changes for the North Atlantic. *Journal of Geophysical Research Oceans*, *113*, C08042. https://doi.org/10.1029/2007JC004501
Rudnick, D. L. (2016). Ocean research enabled by underwater gliders. *Annual Review of Marine Science*. https://doi.org/10.1146/annurev-marine-122414-033913
Rudnick, D. L., & Cole, S. T. (2011). On sampling the ocean using underwater gliders. *Journal of Geophysical Research Oceans*, *116*, C08010. https://doi.org/10.1029/2010JC006849
Sanders, R., Henson, S. A., Koski, M., De La Rocha, C. L., Painter, S. C., Poulton, A. J., et al. (2014). The Biological Carbon Pump in the North Atlantic. *Progress in Oceanography*. https://doi.org/10.1016/j.pocean.2014.05.005
Sarmiento, J. L., Gruber, N., Brzezinski, M. A., & Dunne, J. P. (2004). High-latitude controls of thermocline nutrients and low latitude biological productivity. *Nature*. https://doi.org/10.1038/nature02127
Sarthou, G., Lherminier, P., Achterberg, E. P., Alonso-Pérez, F., Bucciarelli, E., Boutorh, J., et al. (2018). Introduction to the French GEOTRACES North Atlantic transect (GA01): GEOVIDE cruise. *Biogeosciences*. https://doi.org/10.5194/bg-15-7097-2018
Schmid, C. (2014). Mean vertical and horizontal structure of the subtropical circulation in the South Atlantic from three-dimensional observed velocity fields. *Deep Sea Research Part I: Oceanographic Research Papers*. https://doi.org/10.1016/j.dsr.2014.04.015
Schott, F. A., Dengler, M., Zantopp, R., Stramma, L., Fischer, J., & Brandt, P. (2005). The Shallow and Deep Western Boundary Circulation of the South Atlantic at 5°–11°S. *Journal of Physical Oceanography*. https://doi.org/10.1175/JPO2813.1
Sea Bird Electronics, 2014: MicroCAT C-T (P optional) Recorder.
Smeed, D. A., McCarthy, G., Cunningham, S. A., Frajka-Williams, E., Rayner, D., Johns, W. E.,et al. (2014). Observed decline of the Atlantic meridional overturning circulation 2004-2012. *Ocean Science*, *10*(1), 29–38.
Send, U., Davis, R., Fischer, J., Imawaki, S., Kessler, W., Meinen, C., et al. (2010). A global boundary current circulation observing network. *Proceedings of OceanObs'09: Sustained Ocean Observations and Information for Society*. https://doi.org/10.5270/oceanobs09.cwp.78
Send, U., Kanzow, T., Zenk, W., & Rhein, M. (2002). Monitoring the Atlantic Meridional Overturning Circulation at 16°N. *Clivar Exchanges*.
Send, U., Lankhorst, M., & Kanzow, T. (2011). Observation of decadal change in the Atlantic meridional overturning circulation using 10 years of continuous transport data. *Geophysical Research Letters*, *38*, L24606. https://doi.org/10.1029/2011GL049801

Shamberger, K. E. F., Feely, R. A., Sabine, C. L., Atkinson, M. J., DeCarlo, E. H., Mackenzie, F. T., et al. (2011). Calcification and organic production on a Hawaiian coral reef. *Marine Chemistry*. https://doi.org/10.1016/j.marchem.2011.08.003

Shoosmith, D. R., Baringer, M. O., & Johns, W. E. (2005). A continuous record of Florida Current temperature transport at 27°N. *Geophysical Research Letters*, *32*, L23603. https://doi.org/10.1029/2005gl024075

Sigray, P., Lundberg, P., & Döös, K. (2004). Observations of transport variability in the Baltic Sea by parasitic use of a fiber-optic cable. *Journal of Atmospheric and Oceanic Technology*. https://doi.org/10.1175/1520-0426(2004)021<1112:OOTVIT>2.0.CO;2

Sinha, B., Smeed, D. A., McCarthy, G., Moat, B. I., Josey, S. A., Hirschi, J. J.-M., et al. (2018). The accuracy of estimates of the overturning circulation from basin-wide mooring arrays. *Progress in Oceanography*. https://doi.org/10.1016/j.pocean.2017.12.001

Steinfeldt, R., Rhein, M., Bullister, J. L., & Tanhua, T. (2009). Inventory changes in anthropogenic carbon from 1997-2003 in the Atlantic Ocean between 20°S and 65°N. *Global Biogeochemical Cycles*, *23*, GB3010. https://doi.org/10.1029/2008GB003311

Stocker, T. F., Qin, D., Plattner, G.-K., Tignor, M., Allen, S. K., Boschung, J., et al. (2013). *Climate Change 2013: The physical science basis. Contribution of Working Group I to the Fifth Assessment Report of the Intergovernmental Panel on Climate Change*. Cambridge, United Kingdom and New York, NY, USA: Cambridge University Press.

Sverdrup, H. U., Johnson, M. W., & Fleming, R. H. (1942). *The oceans: Their physics, chemistry, and general biology*. New York: Prentice-Hall.

Szuts, Z. B. (2012). Using motionally-induced electric signals to indirectly measure ocean velocity: Instrumental and theoretical developments. *Progress in Oceanography*. https://doi.org/10.1016/j.pocean.2011.11.014

Szuts, Z. B., & Meinen, C. S. (2017). Florida current salinity and salinity transport: Mean and decadal changes. *Geophysical Research Letters*, *44*, 10,495–10,503. https://doi.org/10.1002/2017GL074538

Talley, L. D., Reid, J. L., & Robbins, P. E. (2003). Data-based meridional overturning streamfunctions for the global ocean. *Journal of Climate*, *16*, 3213–3226. https://doi.org/10.1175/1520-0442(2003)016<3213:DMOSFT>2.0.CO;2

Testor, P.,de Young, B.,Rudnick, D. L.,Glenn, S., Hayes, D., Lee, C. M., et al. (2019). OceanGliders: a component of the integrated GOOS. *Frontiers in Marine Science*, *6*(422).

Thurnherr, A. M., Laurent, L. C. S., Speer, K. G., Toole, J. M., & Ledwell, J. R. (2005). Mixing associated with sills in a canyon on the Midocean Ridge Flank*. *Journal of Physical Oceanography*. https://doi.org/10.1175/JPO2773.1

Todd, R. E., Rudnick, D. L., Mazloff, M. R., Davis, R. E., & Cornuelle, B. D. (2011). Poleward flows in the southern California Current System: Glider observations and numerical simulation. *Journal of Geophysical Research Oceans*, *116*, C02026. https://doi.org/10.1029/2010JC006536

Todd, R. E., Rudnick, D. L., Sherman, J. T., Owens, W. B., & George, L. (2017). Absolute velocity estimates from autonomous underwater gliders equipped with Doppler current profilers. *Journal of Atmospheric and Oceanic Technology*. https://doi.org/10.1175/JTECH-D-16-0156.1

Toole, J. M., Andres, M., Le Bras, I. A., Joyce, T. M., & McCartney, M. S. (2017). Moored observations of the Deep Western Boundary Current in the NW Atlantic: 2004–2014. *Journal of Geophysical Research: Oceans*, *122*, 7488–7505. https://doi.org/10.1002/2017JC012984

Toole, J. M., Curry, R. G., Joyce, T. M., McCartney, M., & Peña-Molino, B. (2011). Transport of the North Atlantic Deep Western Boundary Current about 39°N, 70°W: 2004–2008. *Deep Sea Research Part II: Topical Studies in Oceanography*. https://doi.org/10.1016/j.dsr2.2010.10.058

Voet, G., Girton, J. B., Alford, M. H., Carter, G. S., Klymak, J. M., & Mickett, J. B. (2015). Pathways, volume transport, and mixing of abyssal water in the Samoan Passage. *Journal of Physical Oceanography*. https://doi.org/10.1175/JPO-D-14-0096.1

Watson, A. J., Nightingale, P. D., Cooper, D. J., Leach, H., & Follows, M. (1995). Modelling atmosphere-ocean CO transfer. *Philosophical Transactions of the Royal Society B: Biological Sciences*. https://doi.org/10.1098/rstb.1995.0054

Watts, D. R., & Kontoyiannas, H. (1990). Deep-ocean bottom pressure measurement: Drift removal and performance. *Journal of Atmospheric and Oceanic Technology*, *7*, 296–306. https://doi.org/10.1175/1520-0426(1990)007<0296:dobpmd>2.0.co;2

Williams, J., Hughes, C. W., & Tamisiea, M. E. (2015). Detecting trends in bottom pressure measured using a tall mooring and altimetry. *Journal of Geophysical Research, C: Oceans*, *120*, 5216–5232. https://doi.org/10.1002/2015JC010955

Williams, R. G., Roussenov, V., Smith, D., & Lozier, M. S. (2014). Decadal evolution of ocean thermal anomalies in the North Atlantic: The effects of Ekman, overturning, and horizontal transport. *Journal of Climate*, *27*, 698–719. https://doi.org/10.1175/jcli-d-12-00234.1

Willis, J. K. (2010). Can in situ floats and satellite altimeters detect long-term changes in Atlantic Ocean overturning? *Geophysical Research Letters*, *37*, L06602. https://doi.org/10.1029/2010GL042372

Willis, J. K., & Fu, L. L. (2008). Combining altimeter and subsurface float data to estimate the time-averaged circulation in the upper ocean. *Journal of Geophysical Research Oceans*, *113*, C12017. https://doi.org/10.1029/2007JC004690

Worthington, E. L., Frajka-Williams, E., & McCarthy, G. D. (2019). Estimating the deep overturning transport variability at 26°N using bottom pressure recorders. *Journal of Geophysical Research: Oceans*. https://doi.org/10.1029/2018JC014221

Worthington, L. V. (1976). *On the North Atlantic Circulation*. Baltimore: Johns Hopkins University Press.

Wunsch, C. (1996). *The ocean circulation inverse problem*. Cambridge: University Press.

Wunsch, C. (2008). Mass and volume transport variability in an eddy-filled ocean. *Nature Geoscience*, *1*, 165–168. https://doi.org/10.1038/ngeo126

Wust, G. (1935). In W. J. Emery (Ed.), *Schichtung und Zirkulation des Atlantischen Ozeans, Die Stratosphäre. Wissenschaftliche Ergebnisse der Deutschen Atlantischen Expedition auf dem Forschungsund Vermessungsschiff `Meteor' 1925-1927*. E. Translation. Amerind Publishing Co. (1978).

Yashayaev, I., & Loder, J. W. (2016). Recurrent replenishment of Labrador Sea Water and associated decadal-scale variability. *Journal of Geophysical Research: Oceans*, *121*, 8095–8114. https://doi.org/10.1002/2016jc012046

Zantopp, R., Fischer, J., Visbeck, M., & Karstensen, J. (2017). From interannual to decadal: 17 years of boundary current transports at the exit of the Labrador Sea. *J. Geophys. Res. Ocean.*, *122*(3), 1724–1748. https://doi.org/10.1002/2016jc012271C

Zenk, W., & Morozov, E. (2007). Decadal warming of the coldest Antarctic Bottom Water flow through the Vema Channel. *Geophysical Research Letters*, *34*, L14607. https://doi.org/10.1029/2007gl030340

Zhang, R., Sutton, R., Danabasoglu, G., Kwon, Y. O., Marsh, R., Yeager, S. G., et al. (2019). A review of the role of the Atlantic Meridional Overturning Circulation in Atlantic multidecadal variability and associated climate impacts. *Reviews of Geophysics*. https://doi.org/10.1029/2019RG000644

Zweng, M.M, J.R. Reagan, J.I. Antonov, R.A. Locarnini, A.V. Mishonov, T.P. Boyer, et al. 2013: *World Ocean Atlas 2013, Volume 2: Salinity*.